

Survey of Data and Models for Refrigerant Mixtures Containing Halogenated Olefins

Ian H. Bell,* Demian Riccardi, Ala Bazyleva, and Mark O. McLinden

*Applied Chemicals and Materials Division, National Institute of Standards and Technology,
Boulder, CO 80305*

E-mail: ian.bell@nist.gov

Abstract

We survey existing data for refrigerant blends containing halogenated olefins (hydrofluoroolefins (HFO), hydrochlorofluoroolefins (HCFO) and hydrochloroolefins (HCO)) in the open literature. The data are primarily taken from the NIST SOURCE database and are presented in graphical form to demonstrate the relative coverage of the data. The primary conclusion is that blends containing halogenated olefins remain only sparsely measured in experiments, and some classes of data (e.g., speed-of-sound data) are particularly sparse for blends containing halogenated olefins. The second part of this study compares the thermodynamic models in NIST REFPROP against the experimental datasets and identifies systems (of which there are many) where refitting of the thermodynamic model is required.

1 Introduction

The hydrofluoroolefins (HFOs) are a class of refrigerants with very low values of global warming potential (GWP) now coming into use as replacements for the current hydrofluorocarbon (HFC) refrigerants. This is motivated by the Kigali Amendment to the Montreal Protocol, which calls for a 85 % phase down in the GWP-weighted production of the HFCs. “Olefin” refers to a molecule with a carbon-carbon double bond, and HFOs are olefins with selected hydrogens replaced with fluorines. The double

bond is highly reactive to OH radicals in the atmosphere, giving the HFOs very short atmospheric lifetimes of days to weeks compared to years to decades for most of the HFCs. The GWP_{100} (GWP on a 100-year time horizon) of the HFOs is on the order of 1, compared to $GWP_{100} = 1300$ for R-134a, for example.

Many of the HFOs are marginally flammable, with a “2L” flammability classification under ANSI/ASHRAE Standard 34¹ and ISO Standard 817.² Also, as pure fluids, none of the HFOs match the pressure and refrigeration capacity of R-410A, which is a 50/50 (by mass) blend of R-32 (difluoromethane) and R-125 (pentafluoroethane) and is currently the most widely used refrigerant in small air-conditioning systems. Thus, blends of the HFOs with HFCs or other fluids are being investigated as a way to mitigate flammability and/or match the properties of R-410A or other current refrigerants like R-134a.³

Additional candidate refrigerants can be obtained by starting with an olefin and replacing one or more of the hydrogens with any of the halogens (fluorine, chlorine, bromine, iodine) generating the overarching family of halogenated olefins, presently dominated in the commercial sphere by the hydrofluoroolefins. This manipulation yields the refrigerant classes hydrochlorofluoroolefin (HCFO) for olefins with one or more chlorines and one or more fluorines replacing the hydrogens (e.g., R-1224yd(Z)) or hydrochloroolefin (HCO) for olefins with one or more chlorines replacing hydrogens (e.g., R-

1130(E)). While the commercial focus is clearly on HFO, the families of HCFO and HCO include promising working fluids.⁴

A sense of the industrial interest in mixtures containing halogenated olefins can be inferred from the blends classified in ASHRAE Standard 34; as summarized in Fig. 1. The figure is meant to be read like a highway mileage diagram; the full matrix of combinations is symmetric, and the intersection of row and column labels indicate the particular binary mixture. R-444A, the first blend with an HFO, was added to the Standard in January 2013.⁵ In this figure, each binary pair formed of the components of each classified blend is entered once in the counting. For instance, in the ternary mixture of components A, B, and C, the AB, AC, and BC combinations would be counted. The compositions of the components are not considered, so trace components added for improved lubricant compatibility are perhaps over-represented. The classification of a blend in Standard 34 is an early step in the process of commercializing a refrigerant blend because building codes only allow the use of refrigerants included in the standard. Not all of the blends indicated in Fig. 1 will end up being commercialized.

There is, however, a dearth of thermodynamic data on refrigerant blends containing halogenated olefins, and this hinders the development of the mixture models needed for blend selection and equipment design.

Here, we survey the available thermodynamic data for blends containing halogenated olefins and consider the models used to represent those data. In 2018, Bobbo et al.⁶ surveyed the published experimental data for halogenated fluids as pure components and binary mixtures containing halogenated olefins. Their final conclusion of the need for additional experimental measurements aligns with ours. The present study can be seen as an extension of the study of Kayukawa et al.⁷ who surveyed binary blends of five HFOs with ten HFCs and also propane, isobutane, and carbon dioxide. The majority (46 out of 51) were for blends containing R-1234yf or R-1234ze(E). A recent survey⁸ gives an overview of the current state of HFO refrigerants from a variety of standpoints (thermo-

dynamics, heat transfer, etc.). We consider a fairly broad range of fluids as “refrigerants”, and these are listed in Table 1. Included are the most common (as well as some less common) HFCs, a range of the so-called natural refrigerants (hydrocarbons, ammonia, and carbon dioxide), as well as the iodine-containing R-13I1 (trifluoroiodomethane, or CF₃I). Among the halogenated olefins we include the now-common R-1234yf and R-1234ze(E) as well as low-working-pressure refrigerants intended for use with centrifugal compressors (e.g., R-1336mzz(Z)) and fluids in an early stage of development (e.g., R-1123,⁹ R-1132a, R-1132(E), and R-1234ze(Z)). We also include the chlorine-containing HCFOs and HCOs; these fluids have a small, but non-zero ozone-depletion potential (ODP) and are being developed for specialized applications. The table also includes the chemical name as assigned by the International Union of Pure and Applied Chemistry (IUPAC).

We hope that this survey will highlight where additional work is required and also help avoid duplication of effort.

1.1 Alphabet soup (refrigerant nomenclature)

The naming conventions used to describe refrigerants can be somewhat confusing (especially so for halogenated olefins), so a brief summary of the refrigerant numbering conventions is provided here. For refrigerants based upon halogenation of linear alkane molecules, the canonical reference is the ASHRAE Standard 34, with the numbering convention summarized as follows:

- The right-most digit indicates the number of fluorines.
- The second-from-right digit indicates the number of hydrogens plus 1. Atoms attached to the carbon backbone and not otherwise accounted for are assumed to be chlorine.
- The third-from-right digit indicates the number of carbons minus 1 (dropped if the number of carbons is one).

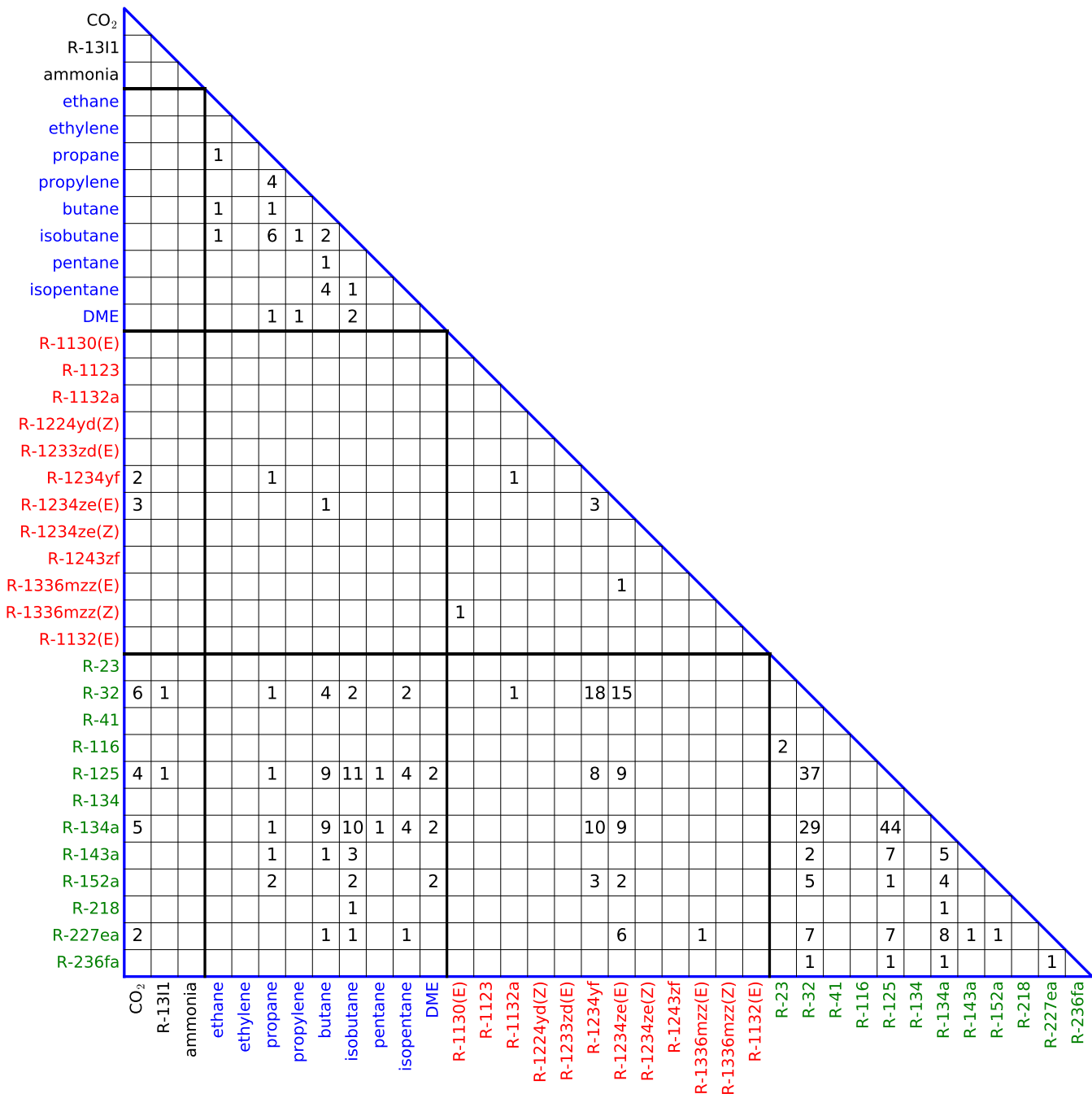


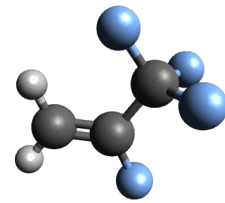
Figure 1: Triangle diagram for coverage of binary pairs in ASHRAE 34 standard for “refrigerants”. Blends containing any components not included in this figure (R-11,R-12,R-13,R-22,R-31,R-115,R-124, or R-142b) were not included in the summation. Each time a binary pair is included in a mixture included in ASHRAE Standard 34, it is included in the summation in this table. The colors correspond to the categories of fluids indicated in Table 1.

Table 1: Pure “refrigerants” considered in this study

name	class	IUPAC chemical name
CO ₂	other	carbon dioxide
R-1311	other	trifluoroiodomethane
ammonia	other	ammonia
ethane	hydrocarbon	ethane
ethylene	hydrocarbon	ethene
propane	hydrocarbon	propane
propylene	hydrocarbon	propene
butane	hydrocarbon	butane
isobutane	hydrocarbon	2-methylpropane
pentane	hydrocarbon	pentane
isopentane	hydrocarbon	2-methylbutane
DME	ether	dimethyl ether
R-1130(E)	HCO	(E)-1,2-dichloroethene
R-1123	HFO	trifluoroethylene
R-1132a	HFO	1,1-difluoroethene
R-1224yd(Z)	HCFO	(Z)-1-chloro-2,3,3,3-tetrafluoro-1-propene
R-1233zd(E)	HCFO	(E)-1-chloro-3,3,3-trifluoro-1-propene
R-1234yf	HFO	2,3,3,3-tetrafluoro-1-propene
R-1234ze(E)	HFO	(E)-1,3,3,3-tetrafluoro-1-propene
R-1234ze(Z)	HFO	(Z)-1,3,3,3-tetrafluoro-1-propene
R-1243zf	HFO	1,1,1-trifluoro-2-propene
R-1336mzz(E)	HFO	(E)-1,1,1,4,4,4-hexafluoro-2-butene
R-1336mzz(Z)	HFO	(Z)-1,1,1,4,4,4-hexafluoro-2-butene
R-1132(E)	HFO	(E)-1,2-difluoroethene
R-23	HFC	trifluoromethane
R-32	HFC	difluoromethane
R-41	HFC	fluoromethane
R-116	FC	hexafluoroethane
R-125	HFC	pentafluoroethane
R-134	HFC	1,1,2,2-tetrafluoroethane
R-134a	HFC	1,1,1,2-tetrafluoroethane
R-143a	HFC	1,1,1-trifluoroethane
R-152a	HFC	1,1-difluoroethane
R-218	FC	octafluoropropane
R-227ea	HFC	1,1,1,2,3,3,3-heptafluoropropane
R-236fa	HFC	1,1,1,3,3,3-hexafluoropropane

- The fourth-from-right digit indicates the number of double bonds, dropped if no double bonds are present; alkene derivatives with a single double-bond will have a number greater than 1000 and less than 2000.
- Additional lowercase letters to the right of the number are used to disambiguate isomers (e.g., the “a” in R-134a to distinguish it from R-134). For 2-carbon molecules the “most-symmetrical” isomer has no appended letter and increasingly asymmetrical molecules have “a”, “b”, etc. appended. For molecules with three or more carbons, the rules are more complicated, and the two or more appended letters designate the atoms attached to different carbons.

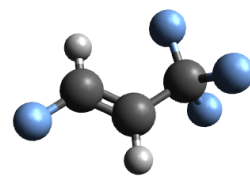
For halogenated olefins, the consideration of conformational isomers (*cis*-/*trans*-) also becomes relevant, and additional modifiers are needed. The *cis*-, or *zusammen*, isomer (German for together), indicated by a suffix of (Z), is for the isomer with the fluorines “together”. The opposite, or *trans*-, isomer is indicated by the suffix (E) for the *entgegen* isomer (German for opposite). Graphical representations of several of the isomers of R-1234 are shown in Fig. 2.



(a) R-1234yf



(b) R-1234ze(Z)



(c) R-1234ze(E)

Figure 2: 3D diagrams of the geometry of R-1234yf and the *cis*- and *trans*- isomers of R-1234ze drawn with Avogadro.¹⁰ Fluorines are blue, hydrogens are grey, and carbons are black.

2 Experimental Data Coverage

The fluids that we categorize as “refrigerants” (see Table 1) are inconsistently studied in experiments; the coverage for mixtures containing halogenated olefins is especially light.

The SOURCE database developed and populated at the Thermodynamics Research Center (National Institute of Standards and Technology) has substantial coverage of the data published in the open literature over the last 15-20 years (i.e., the period when basically all the data on halogenated olefins would have been published). However, the coverage is not complete, and additional data may be found in proprietary sources, conference proceedings, reports, and uncommon journals. Access to the data in SOURCE was made available from an internal interface; data in the SOURCE database are accessible from the NIST ThermoData Engine software package (SRD 103).

In addition to the data available in the SOURCE database, we also carried out ad-

ditional searches for relevant data. In the SciFinder database of the American Chemical Society we searched for papers indexed by the CAS number of any of the most-common HFOs and HCFOs, namely R-1234yf, R-1234ze(E), R-1234ze(Z), R-1233zd(E), and R-1336mzz(Z), mixed either with each other or one of the common HFCs, namely, R-32, R-125, R-134a, R-152a, and R-227ea, for a total of 45 binary pairs. The resulting hits were then further parsed for keywords that would indicate experimental thermodynamic data. We included all types of documents in this search except for patents, which were numerous, but seldom contained useful data. Since the SciFinder database includes CAS numbers, questions of nomenclature are bypassed; however, indexing of the papers lags the addition of new CAS numbers to the database.

In the Fridoc database of the International Institute of Refrigeration, keyword searches (“HFO” AND “mixture”) and (“mixture” AND “thermodynamic property”) were carried out; the hits (which included many papers on heat-transfer behavior and cycle performance, for example) were further parsed. The Fridoc database includes refrigeration conferences that are not typically included in SOURCE. Finally, our sources were compared with those in the surveys of Kayukawa et al.⁷ and Bobbo et al.;⁶ this yielded additional sources, primarily from the quadrennial International Congresses of Refrigeration and Japanese conferences. Some of the sources cited by Kayukawa et al.⁷ did not actually report numerical values, but only a graphical representation, such as points measured.

These searches yielded on the order of 20 additional data references. In some cases we contacted authors and obtained tabular data where only graphical data had been previously published. These data were then added into SOURCE. Thus, we were able to process all of the data in a single workflow.

Figure 3 and Fig. 4 show the data coverage for all experimental measurements on binary refrigerant mixtures included in the NIST SOURCE database for vapor-liquid equilibria (VLE) and density data. Each figure is meant to be read

like a highway mileage diagram; the full matrix of combinations is symmetric, and the intersection of row and column labels indicate the particular binary mixture. The entry in the cell is the total number of data points found. Data points for pure substances included in a set of measurements on a mixture were retained.

Figure 3 shows the number of vapor-liquid-equilibria (VLE) data available for each binary mixture. Each category of fluid (hydrocarbon, halogenated olefin, HFC, other) is indicated by a different color in the axis labels, and are separated by a thick dividing line. This figure shows that the phase equilibria of certain combinations of categories of “refrigerant” mixtures are extensively studied. The binary mixtures of hydrocarbons are of great importance to the natural gas industry (among others), and have been well-measured, accordingly. Mixtures of hydrofluorocarbons (though not all combinations) and refrigerant blends containing hydrofluorocarbons have also seen extensive measurement campaigns.

Unlike other refrigerant class combinations, mixtures containing halogenated olefins have been only sparingly studied in experiments. The only HFOs included in any binary refrigerant mixtures in SOURCE are R-1234yf, R-1234ze(E), R-1234ze(Z), R-1243zf, and R-1336mzz(E). Among these HFOs, only a handful of binary pairs have experimental VLE data (co-existing phase temperature, pressure, and composition data). There are only four HFO+HFO datasets, for the mixtures R-1123+R-1234yf, R-1234ze(E)+R-1234yf, R-1243zf+R-1233ze(E), and R-1234ze(E)+R-1336mzz(E). While we also included HCO- and HCFO-containing blends in our survey, we found no VLE data for such mixtures. The datasets of experimental VLE data for binary mixtures containing HFOs are detailed in Table 2. We limit the discussion here to the HFO-containing mixtures, but all of the datasets referenced in Figs. 3 and 4 are given in Section 4 of the Supporting Information for completeness.

While VLE data are the most important data in defining mixture behavior – they reveal the presence or absence of an azeotrope – density

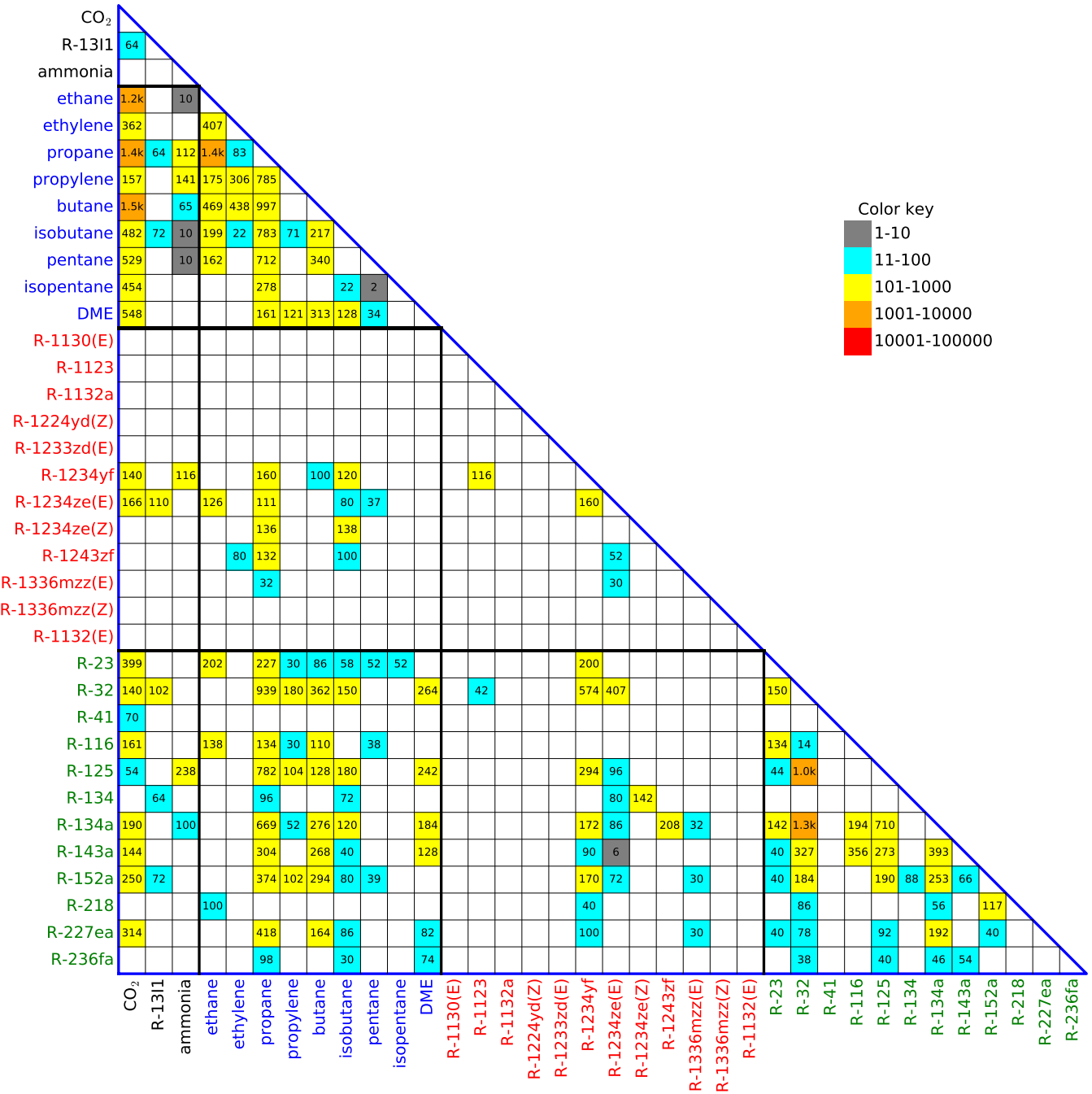


Figure 3: Data point count for VLE measurements for “refrigerants”. Each bubble-point or dew-point measurement is counted individually. The numbers in the individual cells indicate the total number of data points for the binary blend given by the intersection of the row and column.

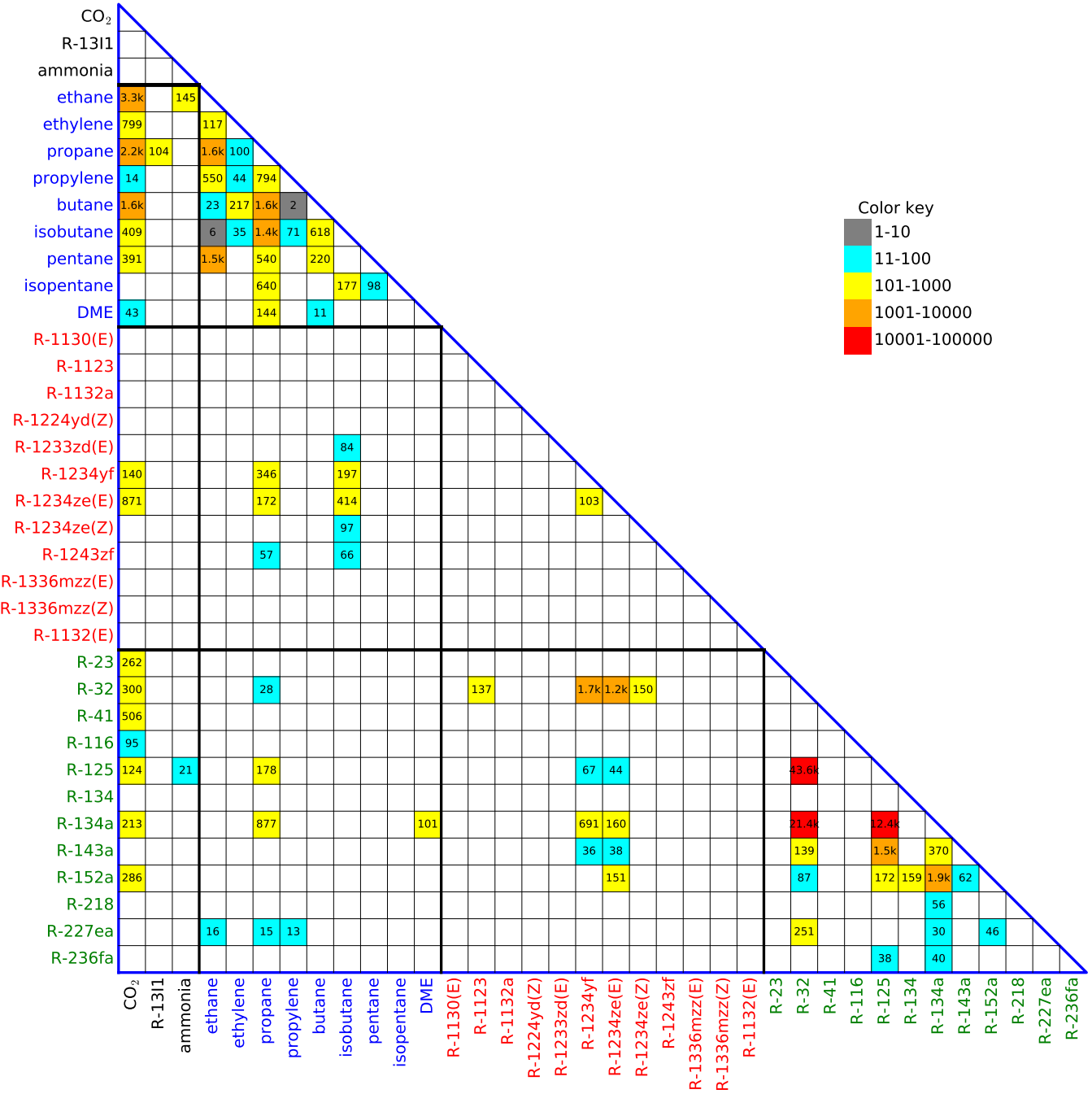


Figure 4: Data point count for density measurements for “refrigerants”. The numbers in the individual cells indicate the total number of data points for the binary blend given by the intersection of the row and column.

Table 2: Data sources for VLE data for the binary mixtures considered in this study. Mole fraction compositions x pertain to the liquid phase, and y to the vapor phase (N_{data} : number of data points).

names (1/2)	reference	year	N_{data}	T / K	x_1	y_1
ammonia/R-1234yf	Zhao et al. ¹¹	2017	58	243.2 - 283.1	0.0 - 1.0	0.0 - 1.0
butane/R-1234yf	Hu et al. ¹²	2018	50	283.1 - 323.1	0.0 - 1.0	0.0 - 1.0
R-13II/R-1234ze(E)	Guo et al. ¹³	2012	55	258.1 - 298.1	0.0 - 1.0	0.0 - 1.0
CO_2 /R-1234yf	Juntarachat et al. ¹⁴	2014	65	283.2 - 353.2	0.0 - 0.9	0.1 - 1.0
CO_2 /R-1234yf	Arami-Niya et al. ¹⁵	2020	5	293.0 - 293.1	0.1 - 0.6	0.3 - 0.9
CO_2 /R-1234ze(E)	Wang et al. ¹⁶	2019	83	283.3 - 353.0	0.0 - 1.0	0.0 - 1.0
ethane/R-1234ze(E)	Liu et al. ¹⁷	2018	63	272.3 - 347.5	0.0 - 0.9	0.1 - 1.0
ethylene/R-1243zf	Zernov et al. ¹⁸	1971	40	283.1 - 363.1	0.0 - 0.9	0.0 - 1.0
isobutane/R-1234yf	Hu et al. ¹⁹	2014	60	283.1 - 323.1	0.0 - 1.0	0.0 - 1.0
isobutane/R-1234ze(E)	Dong et al. ²⁰	2012	40	258.1 - 288.1	0.0 - 1.0	0.0 - 1.0
isobutane/R-1234ze(Z)	Zhang et al. ²¹	2016	69	303.1 - 353.1	0.0 - 1.0	0.0 - 1.0
isobutane/R-1243zf	Deng et al. ²²	2020	50	253.2 - 293.1	0.0 - 1.0	0.0 - 1.0
pentane/R-1234ze(E)	Outcalt and Lemmon ²³	2013	37	269.9 - 380.0	0.3 - 0.7	
propane/R-1234yf	Zhong et al. ²⁴	2017	55	253.2 - 293.1	0.0 - 1.0	0.0 - 1.0
propane/R-1234yf	Zhong et al. ²⁵	2018	50	255.0 - 300.1	0.4 - 0.9	
propane/R-1234ze(E)	Dong et al. ²⁶	2011	38	258.1 - 283.1	0.0 - 1.0	0.0 - 1.0
propane/R-1234ze(E)	Zhang et al. ²⁷	2016	35	253.1 - 293.3	0.1 - 0.8	
propane/R-1234ze(Z)	Gong et al. ²⁸	2016	68	253.2 - 293.1	0.0 - 1.0	0.0 - 1.0
propane/R-1243zf	Ding et al. ²⁹	2020	66	243.2 - 288.1	0.0 - 1.0	0.0 - 1.0
propane/R-1336mzz(E)	Boonaert et al. ³⁰	2020	16	313.2 - 353.1	0.1 - 0.8	0.3 - 0.9
R-1123/R-1234yf	Miyamoto et al. ³¹	2021	98	300.0 - 330.0	0.1 - 0.7	0.2 - 0.8
R-1234yf/R-1234ze(E)	Al Ghafri et al. ³²	2019	3	273.6 - 341.7	0.7 - 0.7	0.7 - 0.7
R-1234yf/R-1234ze(E)	Ye et al. ³³	2021	77	283.6 - 333.4	0.0 - 1.0	0.0 - 1.0
R-1234ze(E)/R-1336mzz(E)	Boonaert et al. ³⁰	2020	15	313.2 - 353.1	0.2 - 0.9	0.3 - 0.9
R-1243zf/R-1234ze(E)	Yang et al. ³⁴	2020	52	293.0 - 353.0	0.1 - 0.9	0.1 - 0.9
R-125/R-1234yf	Kamiaka et al. ³⁵	2010	28	273.3 - 333.1	0.2 - 0.5	0.3 - 0.7
R-125/R-1234yf	Kamiaka et al. ³⁶	2013	84	273.3 - 333.2	0.0 - 1.0	0.0 - 1.0
R-125/R-1234yf	Yang et al. ³⁷	2020	35	283.1 - 323.1	0.0 - 1.0	0.0 - 1.0
R-125/R-1234ze(E)	Al Ghafri et al. ³²	2019	3	274.5 - 341.7	0.5 - 0.5	0.6 - 0.7
R-125/R-1234ze(E)	Yang et al. ³⁷	2020	45	283.1 - 323.1	0.0 - 1.0	0.0 - 1.0
R-134/R-1234ze(E)	Dong et al. ³⁸	2013	40	258.1 - 288.1	0.0 - 1.0	0.0 - 1.0
R-134/R-1234ze(Z)	Zhang et al. ³⁹	2017	71	303.1 - 343.1	0.0 - 1.0	0.0 - 1.0
R-134a/R-1234yf	Shimoura et al. ⁴⁰	2011	5	283.1 - 313.1	0.6	
R-134a/R-1234yf	Kamiaka et al. ³⁶	2013	67	273.3 - 333.2	0.0 - 1.0	0.0 - 1.0
R-134a/R-1234yf	Chen et al. ⁴¹	2016	41	268.2 - 323.2	0.5 - 0.6	
R-134a/R-1234ze(E)	Al Ghafri et al. ³²	2019	3	273.5 - 340.6	0.5 - 0.5	0.5 - 0.6
R-134a/R-1234ze(E)	Kou et al. ⁴²	2019	40	293.1 - 323.1	0.0 - 1.0	0.0 - 1.0
R-134a/R-1243zf	Yang et al. ⁴³	2019	44	293.1 - 323.1	0.0 - 1.0	0.0 - 1.0
R-134a/R-1243zf	Yao et al. ⁴⁴	2020	60	243.2 - 293.1	0.0 - 1.0	0.0 - 1.0
R-134a/R-1336mzz(E)	Boonaert et al. ³⁰	2020	16	313.2 - 353.1	0.1 - 0.8	0.3 - 0.9
R-143a/R-1234yf	Hu et al. ⁴⁵	2013	45	283.1 - 323.1	0.0 - 1.0	0.0 - 1.0
R-143a/R-1234ze(E)	Al Ghafri et al. ³²	2019	3	274.3 - 340.4	0.5 - 0.5	0.6 - 0.7
R-152a/R-1234yf	Hu et al. ⁴⁶	2014	60	283.1 - 323.1	0.0 - 1.0	0.0 - 1.0
R-152a/R-1234yf	Yang et al. ⁴⁷	2018	25	283.1 - 323.1	0.0 - 1.0	0.0 - 1.0
R-152a/R-1234ze(E)	Yang et al. ⁴⁸	2013	36	258.1 - 288.1	0.1 - 0.9	0.1 - 0.9
R-152a/R-1336mzz(E)	Boonaert et al. ³⁰	2020	15	313.2 - 353.1	0.1 - 0.9	0.2 - 0.9
R-218/R-1234yf	Kochenburger et al. ⁴⁹	2017	20	223.1 - 272.8	0.0 - 1.0	0.0 - 1.0
R-227ea/R-1234yf	Hu et al. ⁵⁰	2014	50	283.1 - 323.1	0.0 - 1.0	0.0 - 1.0
R-227ea/R-1336mzz(E)	Boonaert et al. ³⁰	2020	15	313.2 - 353.1	0.1 - 0.8	0.2 - 0.9
R-23/R-1234yf	Madani et al. ⁵¹	2016	74	254.1 - 348.4	0.0 - 0.9	0.0 - 1.0
R-23/R-1234yf	Kochenburger et al. ⁴⁹	2017	26	193.2 - 273.2	0.0 - 1.0	0.0 - 1.0
R-32/R-1123	Miyamoto et al. ⁵²	2020	21	273.5 - 330.1	0.3 - 0.8	0.3 - 0.7
R-32/R-1234yf	Kamiaka et al. ³⁵	2010	35	273.3 - 333.1	0.3 - 0.8	0.5 - 0.9
R-32/R-1234yf	Kobayashi et al. ⁵³	2011	11	347.8 - 359.7	0.4 - 0.7	0.4 - 0.7
R-32/R-1234yf	Shimoura et al. ⁴⁰	2011	5	283.1 - 313.1	0.6	
R-32/R-1234yf	Kamiaka et al. ³⁶	2013	79	273.3 - 333.1	0.0 - 1.0	0.0 - 1.0
R-32/R-1234yf	Hu et al. ⁵⁴	2017	55	283.1 - 323.1	0.0 - 1.0	0.0 - 1.0
R-32/R-1234yf	Al Ghafri et al. ³²	2019	3	273.7 - 340.9	0.8 - 0.8	0.8 - 0.9
R-32/R-1234yf	Yamada et al. ⁵⁵	2020	53	283.1 - 329.9	0.1 - 0.8	0.2 - 0.8
R-32/R-1234yf	Li et al. ⁵⁶	2021	77	273.1 - 358.1	0.0 - 1.0	0.0 - 1.0
R-32/R-1234ze(E)	Kobayashi et al. ⁵⁷	2011	14	358.1 - 371.5	0.4 - 0.7	0.4 - 0.7
R-32/R-1234ze(E)	Tanaka et al. ⁵⁸	2011	10	310.0 - 350.0	0.4 - 0.7	
R-32/R-1234ze(E)	Akasaka ⁵⁹	2013	151	272.9 - 314.0	0.1 - 0.9	0.2 - 1.0
R-32/R-1234ze(E)	Hu et al. ⁶⁰	2017	65	283.1 - 323.1	0.0 - 1.0	0.0 - 1.0
R-32/R-1234ze(E)	Hu et al. ⁵⁴	2017	15	283.1 - 323.1	0.2 - 0.7	0.3 - 0.9
R-32/R-1234ze(E)	Kou et al. ⁴²	2019	36	293.1 - 323.1	0.0 - 1.0	0.0 - 1.0

Table 3: Data sources for p - ρ - T data for the binary mixtures considered in this study. Mole fraction compositions x pertain to the bulk phase (N_{data} : number of data points).

names (1/2)	reference	year	N_{data}	T / K	x_1
CO ₂ /R-1234yf	Di Nicola et al. ⁶¹	2012	128	223.1 - 372.9	0.1 - 0.8
CO ₂ /R-1234yf	Arami-Niya et al. ¹⁵	2020	12	233.2 - 303.1	0.5
CO ₂ /R-1234ze(E)	Yamaya et al. ⁶²	2010	39	270.1 - 425.1	0.5
CO ₂ /R-1234ze(E)	Yamaya et al. ⁶³	2011	39	270.1 - 425.1	0.5
CO ₂ /R-1234ze(E)	Di Nicola et al. ⁶⁴	2013	112	233.1 - 363.1	0.2 - 0.9
CO ₂ /R-1234ze(E)	Fu et al. ⁶⁵	2020	681	283.0 - 353.1	0.2 - 0.8
isobutane/R-1233zd(E)	Brown et al. ⁶⁶	2018	84	303.1 - 383.1	0.1 - 0.9
isobutane/R-1234yf	Brown et al. ⁶⁷	2017	96	303.1 - 383.1	0.2 - 0.8
isobutane/R-1234yf	Zhang et al. ⁶⁸	2018	101	270.1 - 300.2	0.1 - 0.7
isobutane/R-1234ze(E)	Brown et al. ⁶⁷	2017	102	303.1 - 383.1	0.3 - 0.8
isobutane/R-1234ze(E)	Cao et al. ⁶⁹	2017	312	280.2 - 330.2	0.2 - 0.5
isobutane/R-1234ze(Z)	Brown et al. ⁶⁶	2018	97	303.1 - 383.1	0.1 - 0.7
isobutane/R-1243zf	Tomassetti et al. ⁷⁰	2019	66	303.1 - 383.1	0.2 - 0.9
propane/R-1234yf	Brown et al. ⁷¹	2016	86	268.1 - 363.2	0.2 - 0.8
propane/R-1234yf	Zhong et al. ⁷²	2017	168	265.5 - 300.3	0.0 - 0.9
propane/R-1234yf	Zhong et al. ²⁵	2018	50	255.0 - 300.1	0.4 - 0.9
propane/R-1234yf	Zhong et al. ⁷³	2019	42	254.3 - 348.3	0.2 - 0.7
propane/R-1234ze(E)	Zhang et al. ⁷⁴	2016	137	258.1 - 293.4	0.1 - 0.8
propane/R-1234ze(E)	Zhang et al. ²⁷	2016	35	253.1 - 293.3	0.1 - 0.8
propane/R-1243zf	Sheng et al. ⁷⁵	2020	57	292.8 - 349.4	0.2 - 0.8
R-1234yf/R-1234ze(E)	Higashi ⁷⁶	2015	14	354.6 - 374.3	0.5
R-1234yf/R-1234ze(E)	Higashi ⁷⁷	2016	52	340.0 - 430.0	0.5
R-1234yf/R-1234ze(E)	Al Ghafri et al. ³²	2019	37	252.2 - 403.5	0.5
R-125/R-1234yf	Dang et al. ⁷⁸	2015	27	283.6 - 318.0	0.3 - 0.7
R-125/R-1234yf	Al Ghafri et al. ³²	2019	40	252.1 - 382.9	0.5
R-125/R-1234ze(E)	Al Ghafri et al. ³²	2019	44	252.1 - 383.9	0.5
R-134a/R-1234yf	Yotsumoto et al. ⁷⁹	2010	575	263.1 - 323.1	0.0 - 0.8
R-134a/R-1234yf	Akasaka et al. ⁸⁰	2015	22	350.3 - 370.7	0.3 - 0.7
R-134a/R-1234yf	Chen et al. ⁸¹	2015	94	298.6 - 403.2	0.0 - 0.9
R-134a/R-1234ze(E)	Zhang et al. ⁸²	2017	101	270.4 - 300.3	0.4 - 0.6
R-134a/R-1234ze(E)	Al Ghafri et al. ³²	2019	59	252.1 - 403.4	0.5
R-143a/R-1234yf	Al Ghafri et al. ³²	2019	36	252.2 - 363.2	0.5
R-143a/R-1234ze(E)	Al Ghafri et al. ³²	2019	38	252.0 - 383.0	0.5
R-152a/R-1234ze(E)	Qi et al. ⁸³	2020	151	285.3 - 310.2	0.6 - 0.8
R-32/R-1123	Higashi and Akasaka ⁸⁴	2016	137	310.0 - 430.0	0.5 - 0.7
R-32/R-1234yf	Akatsu et al. ⁸⁵	2011	40	332.8 - 363.6	0.2 - 0.7
R-32/R-1234yf	Kobayashi et al. ⁵³	2011	295	310.0 - 395.0	0.4 - 0.7
R-32/R-1234yf	Akasaka et al. ⁸⁶	2013	40	332.8 - 363.6	0.2 - 0.7
R-32/R-1234yf	Dang et al. ⁷⁸	2015	26	283.4 - 318.6	0.5 - 0.8
R-32/R-1234yf	Cai et al. ⁸⁷	2018	153	279.8 - 347.9	0.4 - 0.9
R-32/R-1234yf	Yang et al. ⁸⁸	2019	492	298.8 - 383.1	0.1 - 0.9
R-32/R-1234yf	Jia et al. ⁸⁹	2020	485	283.5 - 363.2	0.2 - 0.9
R-32/R-1234yf	Tomassetti et al. ⁹⁰	2020	217	263.1 - 383.1	0.1 - 0.9
R-32/R-1234ze(E)	Kobayashi et al. ⁹¹	2010	23	341.2 - 371.8	0.4 - 0.7
R-32/R-1234ze(E)	Kobayashi et al. ⁵⁷	2011	330	310.0 - 400.0	0.4 - 0.7
R-32/R-1234ze(E)	Tanaka et al. ⁵⁸	2011	81	310.0 - 350.0	0.4 - 0.7
R-32/R-1234ze(E)	Yamaya et al. ⁹²	2011	47	280.1 - 460.1	0.7
R-32/R-1234ze(E)	Jia et al. ⁹³	2016	540	283.5 - 362.7	0.2 - 1.0
R-32/R-1234ze(E)	Tomassetti et al. ⁹⁴	2020	182	263.1 - 373.1	0.2 - 1.0
R-32/R-1234ze(Z)	Tomassetti et al. ⁹⁵	2020	150	263.1 - 373.1	0.1 - 0.9

(p, ρ, T, x) data are also important for model development. The Helmholtz energy is a function of temperature and density, and most VLE datasets provide no density information. The calculation of other thermodynamic properties, including enthalpy, entropy, and heat capacity, which are important in cycle analysis, involve derivatives of the density. Figure 4 shows the coverage of density data. The experimental data coverage for HFO-containing blends is even more limited than VLE; only 22 HFO-containing blends and one HCFO-containing blend have any experimental p - ρ - T data. Generally, in contrast to fitting either homogeneous phase density or phase equilibria data individually, which is generally straightforward, fitting both simultaneously tends to be challenging. Mixture model predictions are unreliable when fitted exclusively to VLE data, an unfortunately common practice. This point is further explored below. The datasets of experimental p - ρ - T data for binary mixtures containing HFOs are detailed in Table 3.

There are a small number of other kinds of thermodynamic data for HFO-containing blends, as listed in Table 4. We were only able to identify a single speed-of-sound dataset⁴⁰ for HFO-containing blends in the open literature; speed of sound data is crucial for the development of high accuracy pure fluid equations of state and would also be useful for development of high-accuracy mixture models. Speed of sound measurements are instrumental because they can be carried out with very low uncertainty (expected relative expanded combined uncertainty ($k=2$) on the order of 0.02 %, see as an example Ref. 96). Speed of sound measurements provide strong constraints on the caloric properties, which are otherwise not usually as accurately predicted by EOS. In light of the clear gaps in the experimental data coverage for binary mixtures including halogenated olefins, there are ongoing efforts at several institutions globally, including ours, to conduct new reference-quality measurements.

Table 4: Other thermodynamic data for the binary mixtures containing halogenated olefins considered in this study (N_{data} : number of data points, c_p : constant pressure heat capacity, c_v : constant volume heat capacity, T_c : critical temperature, p_c : critical pressure, v_c : critical volume, w : speed of sound).

property	names (1/2)	reference	year	N_{data}
T_c	R-32/R-1234yf	Akasaka et al. ⁸⁶	2013	3
p_c	R-32/R-1234yf	Akasaka et al. ⁸⁶	2013	3
v_c	R-32/R-1234yf	Akasaka et al. ⁸⁶	2013	3
c_p	R-32/R-1234yf	Al Ghafri et al. ³²	2019	1
w	R-32/R-1234yf	Shimoura et al. ⁴⁰	2011	92
c_p	R-1234yf/R-1234ze(E)	Al Ghafri et al. ³²	2019	1
T_c	R-1234yf/R-1234ze(E)	Higashi ⁷⁷	2016	1
p_c	R-1234yf/R-1234ze(E)	Higashi ⁷⁷	2016	1
v_c	R-1234yf/R-1234ze(E)	Higashi ⁷⁷	2016	1
T_c	R-1234yf/R-134a	Akasaka et al. ⁸⁰	2015	3
v_c	R-1234yf/R-134a	Akasaka et al. ⁸⁰	2015	3
p_c	R-1234yf/R-134a	Akasaka et al. ⁸⁰	2015	3
w	R-1234yf/R-134a	Shimoura et al. ⁴⁰	2011	93
c_p	R-32/R-1234ze(E)	Gao et al. ⁹⁷	2018	25
c_p	R-32/R-1234ze(E)	Tanaka et al. ⁵⁸	2011	38
c_v	R-32/R-1234ze(E)	Yamaya et al. ⁹²	2011	47
p_c	R-32/R-1234ze(E)	Kobayashi et al. ⁵⁷	2011	2
T_c	R-32/R-1234ze(E)	Kobayashi et al. ⁵⁷	2011	2
v_c	R-32/R-1234ze(E)	Kobayashi et al. ⁵⁷	2011	2
p_c	ethylene/R-1243zf	Zernov et al. ¹⁸	1971	6
T_c	ethylene/R-1243zf	Zernov et al. ¹⁸	1971	6
c_p	R-125/R-1234ze(E)	Al Ghafri et al. ³²	2019	1
c_p	R-134a/R-1234ze(E)	Al Ghafri et al. ³²	2019	1
c_p	R-143a/R-1234ze(E)	Al Ghafri et al. ³²	2019	1
c_p	R-143a/R-1234yf	Al Ghafri et al. ³²	2019	1
c_p	R-125/R-1234yf	Al Ghafri et al. ³²	2019	1
c_v	propane/R-1234yf	Zhong et al. ⁷³	2019	89
c_v	CO ₂ /R-1234ze(E)	Yamaya et al. ⁶²	2010	39
T_c	CO ₂ /R-1234ze(E)	Juntarachat et al. ¹⁴	2014	11
p_c	CO ₂ /R-1234ze(E)	Juntarachat et al. ¹⁴	2014	11
c_v	CO ₂ /R-1234ze(E)	Yamaya et al. ⁶³	2011	39
T_c	CO ₂ /R-1234yf	Juntarachat et al. ¹⁴	2014	11
p_c	CO ₂ /R-1234yf	Juntarachat et al. ¹⁴	2014	11
c_p	CO ₂ /R-1234yf	Arami-Niya et al. ¹⁵	2020	9
c_v	propane/R-1243zf	Sheng et al. ⁷⁵	2020	82
T_c	R-1123/R-32	Higashi and Akasaka ⁸⁴	2016	4
p_c	R-1123/R-32	Higashi and Akasaka ⁸⁴	2016	4
v_c	R-1123/R-32	Higashi and Akasaka ⁸⁴	2016	4
T_c	R-23/R-1234yf	Madani et al. ⁵¹	2016	4
p_c	R-23/R-1234yf	Madani et al. ⁵¹	2016	4

3 Models

3.1 Modeling approaches

Due to the broad spectrum of modeling approaches that have been considered for blends containing halogenated olefins, any survey will be necessarily incomplete. Equation of state approaches have included group-contribution volume translated Peng-Robinson (GC-VTPR),^{98–102} perturbed-chain polar SAFT,^{103,104} cubic plus association (CPA)^{105,106} and predictive Peng-Robinson (PPR78).^{14,107} With very few exceptions, insufficient detail is provided in the literature to verify the performance of the proposed equations of state. While these models can in many cases provide adequate representation of the vapor-liquid-equilibrium (especially the cubic equations of state), simultaneously representing all thermodynamic properties with a consistent model formulation is challenging. For that reason, the most accurate property predictions are obtained from properly-tuned multi-fluid Helmholtz-energy based thermodynamic models.^{108,109}

While not precisely in the same vein of thermodynamic modeling, molecular dynamics studies have also been carried out, for instance the molecular dynamics studies of Raabe.^{110–113} This molecular simulation data is complementary to experimental data, for instance molecular simulation results¹¹⁴ were included in the model development work of Akasaka⁵⁹ for R-32 mixed with R-1234yf and R-1234ze(E).

3.2 Multi-Fluid Modeling

While there are a variety of modeling approaches for mixtures containing halogenated olefins, a comparison of these models is outside the scope of the present paper. Rather, we will consider here only the mixture models implemented in NIST REFPROP version 10.0.0.2.¹¹⁵ We will use deviations between the data and the REFPROP models to compare different data sets with each other and to draw general conclusions regarding the adequacy of those models and where further modeling work may be

needed.

The thermodynamic mixture models implemented in NIST REFPROP, which can be referred to as multi-fluid models, combine accurate equations of state for the pure components with reducing functions and optionally, so-called departure functions, which can be either specific to a particular binary pair or generalized functions applicable to a class of mixtures. The reduced Helmholtz energy $\alpha = a/(RT)$ of the mixture is given by summations over the N components of the mixture

$$\alpha = \sum_{i=1}^N x_i [\alpha_i^0(\tau, \delta) + \ln x_i + \alpha_i^r(\tau, \delta)] + \sum_{i=1}^{N-1} \sum_{j=i+1}^N x_i x_j F_{ij} \alpha_{ij}^E(\tau, \delta) \quad (1)$$

where the α_i^0 terms are the ideal-gas parts of the pure-fluid EOS for each of the N mixture components. The $\ln x_i$ terms arise from the entropy of mixing. The α_i^r are the “residual” or “real-gas” parts of each of the component EOS. The α_{ij}^E is a departure function and F_{ij} is a binary-specific multiplier.

The α_i^r and α_{ij}^E are not evaluated at the mixture T and ρ , but rather, at the mixture reduced density $\delta = \rho/\rho_r(\bar{x})$ which is a function of the mole fraction composition array \bar{x} and the reciprocal reduced temperature $\tau = T_r(\bar{x})/T$, with the reducing functions given by

$$T_r(\bar{x}) = \sum_{i=1}^N x_i^2 T_{c,i} + \sum_{i=1}^{N-1} \sum_{j=i+1}^N 2x_i x_j \frac{x_i + x_j}{\beta_{T,ij}^2 x_i + x_j} T_{ij} \quad (2)$$

$$v_r(\bar{x}) = \sum_{i=1}^N x_i^2 v_{c,i} + \sum_{i=1}^{N-1} \sum_{j=i+1}^N 2x_i x_j \frac{x_i + x_j}{\beta_{v,ij}^2 x_i + x_j} v_{ij} \quad (3)$$

with

$$T_{ij} = \beta_{T,ij} \gamma_{T,ij} (T_{c,i} T_{c,j})^{0.5} \quad (4)$$

$$v_{ij} = \frac{1}{8} \beta_{v,ij} \gamma_{v,ij} \left(v_{c,i}^{1/3} + v_{c,j}^{1/3} \right)^3 \quad (5)$$

where $T_{c,i}$ and $v_{c,i}$ are the critical temperature and critical volume of the i -th component, re-

spectively. These mixture reducing equations are weighted averages of the critical properties of the mixture components, with four adjustable parameters per ij binary pair: $\beta_{T,ij}$, $\gamma_{T,ij}$, $\beta_{v,ij}$, and $\gamma_{v,ij}$.

The fitted interaction parameters (along with the F_{ij} when present) are listed in Table 5 for the models currently implemented in REFPROP 10.0. When an alternative pair is in use for estimation, the asymmetric parameters $\beta_{T,ij} = 1/\beta_{T,ji}$ and $\beta_{v,ij} = 1/\beta_{v,ji}$ do not necessarily match the alternative pair order, but the symmetric parameters $\gamma_{T,ij}$ and $\gamma_{T,ji}$ are not sensitive to ordering. Cross-validation calculations with CoolProp 6.4.1¹¹⁶ yield agreement for the check values within 0.001% in all cases. Fluids in a given binary pair are sorted by normal boiling point temperature in order to be consistent with the file of interaction parameters (i.e., the `HMX.BNC` file) of REFPROP 10.0. Many of the fitting parameters come from the automatic fitting of Bell and Lemmon.¹¹⁷ That work, published in 2016, does not include any experimental data captured after approximately mid-2015. To maintain consistency in the refrigeration industry, some parameters previously fit to unpublished and proprietary experimental data or molecular simulation results (the UNP models in Table 5) were not updated in REFPROP 10.0, even though newer published data supercede the previous data, and coefficients were provided in Bell and Lemmon.¹¹⁷

When no experimental data are available but estimated interaction parameters are required, two schemes are in use. The historical method is that of Lemmon and McLinden,¹¹⁸ used to estimate interaction parameters for HFC-containing blends. A newer method implemented in REFPROP 10.0 is to use the interaction parameters for “similar” binary pairs. The estimation scheme employed is indicated in Table 5.

3.3 VLE

Figure 5 shows all the VLE data for olefin-containing blends, colored by the temperature, in a pressure-composition representation. The intention of putting all the data into one figure

at a very small printed size is to give a high-level overview. In order to make the data and models legible, much larger figures for each binary pair are in Section 1 of the Supporting Information. An automated means is needed to determine the isotherms that should be plotted, which is complicated by the fact that some authors present the temperature of the nominal isotherm, and others the as-measured temperature. A kernel density estimation method was used to obtain a reasonable set of isotherms. These isotherms were traced with the method of Bell and Deiters.¹¹⁹ The solid curves are the model-predicted values of the isothermal cross-sections of the phase envelope. In most cases, the model yields at least a qualitatively accurate representation of the experimental data. In some cases where estimation has been used (indicated by an E in the upper right-corner), the presence of an azeotrope was correctly identified, but the strength of the azeotrope was missed. The model for the binary mixture of R-13I1 + R-1234ze(E) was discussed in a recent publication.¹²⁰ The estimation scheme for refrigerant interaction parameters should not be used with ammonia^a. EOS for R-134 and R-1336mzz(E) are not available in REFPROP 10.0. Thus, we do not draw isotherms for mixtures containing ammonia, R-134, or R-1336mzz(E).

Quantifying the accuracy of VLE predictions from mixture models is not straightforward. At low pressure, deviations in pressure are meaningful, and in parts of the critical region, deviations in composition are more meaningful because the slope of isotherm (in the coordinates of the plot) goes to infinity. For that reason, orthogonal distance between a point and the phase envelope has been used as an error metric in other works.¹²¹ Here, we consider only pressure deviations, emphasizing that near-critical model predictions will be unfairly penalized by this error metric. We further emphasize that

^aThe estimation scheme does not yield a sensible model prediction for ammonia + R-1234yf; the estimation scheme yields a negative pressure azeotrope (uncommon for refrigerant blends), while the experimental data show the presence of a positive pressure azeotrope (much more common)

Table 5: Binary interaction parameters used in REFPROP 10.0 for blends with VLE or density data. Check value p_{chk} (calculated with REFPROP 10.0), is the bubble-point pressure at 298 K and a mole fraction given by $x_1 = 0.4$.

names (1/2)	ref. [†]	est. [‡]	$\beta_{T,12}$	$\gamma_{T,12}$	$\beta_{v,12}$	$\gamma_{v,12}$	F_{ij}^*	$p_{\text{chk}} / \text{MPa}$
CO ₂ /R-1234yf	UNP		1.017	1	1	1.015	-0.657 (KW0)	2.44362
CO ₂ /R-1234ze(E)	UNP		1	1.023	1	1	-0.084 (KW0)	2.15977
R-13H/R-1234ze(E)	LM		0.949822	1	1.00009			0.59256
ethane/R-1234ze(E)	LM		0.912325	1	1.01825			2.58705
ethylene/R-1243zf	LM		0.940888	1	1.02732			3.30544
propane/R-1234yf	LM		0.962174	1	1.00274			0.894306
propane/R-1234ze(E)	LM		0.943774	1	1.00195			0.841683
propane/R-1243zf	LM		0.95395	1	1.00415			0.622348
isobutane/R-1233zd(E)	R1234yf/Isobutane	1.0073	0.93536	1	1			0.827158
isobutane/R-1234ze(Z)	LM	1	0.965644	1	1.00189			0.306485
R-1234yf/butane	R1234yf/Isobutane	0.992753	0.93536	1	1			0.311839
R-1234yf/isobutane	117	0.992753	0.93536	1	1			0.542571
R-1234yf/R-1234ze(E)	UNP	1	0.951434	1	1.00008			0.614172
R-1234yf/R-134a	UNP	1	0.987	1	1			0.600222
R-1234yf/R-152a	117	0.9963	0.98112	1	1			0.707141
R-1234yf/R-227ea	117	0.99938	0.99916	1	1			0.671841
R-1234ze(E)/isobutane	R1234yf/Isobutane	0.992753	0.93536	1	1			0.543462
R-1243ze(E)/pentane	UNP	1.00705	0.937	1	1			0.34522
R-1243zf/isobutane	R1234yf/R1234ze(E)	0.992753	0.93536	1	1			0.569169
R-1243zf/R-1234ze(E)	LM	1	1.01	1	1			0.560467
R-23/R-1234yf	R-32/R-1234yf	59	1.00052	0.948538	0.993346	1.02211	-0.277708 (KW4)	1.21041
R-32/R-1234ze(E)	59	1.00343	0.977857	1.00586	0.982707	-0.265419 (KW2)	1.02885	
R-32/R-1234ze(Z)	R32/R1234ze(E)	1.00343	0.977857	1.00586	0.982707	-0.265419 (KW2)	0.846399	
R-125/R-1234yf	UNP	1	0.999	1	1			0.945332
R-125/R-1234ze(E)	UNP	1.003	1.0071	1	1			0.812898
R-134a/R-1234ze(E)	UNP	1	0.992	1	1			0.579216
R-134a/R-1243zf	R1234yf/R134a	1	0.985	1	1			0.651219
R-143a/R-1234yf	117	0.99976	0.99523	1	1			0.916598
R-143a/R-1234ze(E)	R143a/R1234yf	0.99976	0.99523	1	1			0.809876
R-152a/R-1234ze(E)	R1234yf/R152a	1.00371	0.98112	1	1			0.572041
R-218/R-1234yf	LM	1	0.983655	1	1.0041			0.792016
R-1123/R-1234yf	R1234yf/R1234ze(E)	1	0.987	1	1			1.263398
R-1123/R-32	R32/R1234yf	0.99948	0.948538	1.0067	1.02211	-0.277708 (KW4)	2.14622	

[†] UNP: unpublished model [‡] LM: estimation scheme of Lemmon and McLinden;¹¹⁸ pair of names: alternative pair used to estimate interaction parameters *: The departure function (KW_x, x being a placeholder) is named according to the models used in REFFPROP. If the value of F_{ij} is zero, no departure function is used.

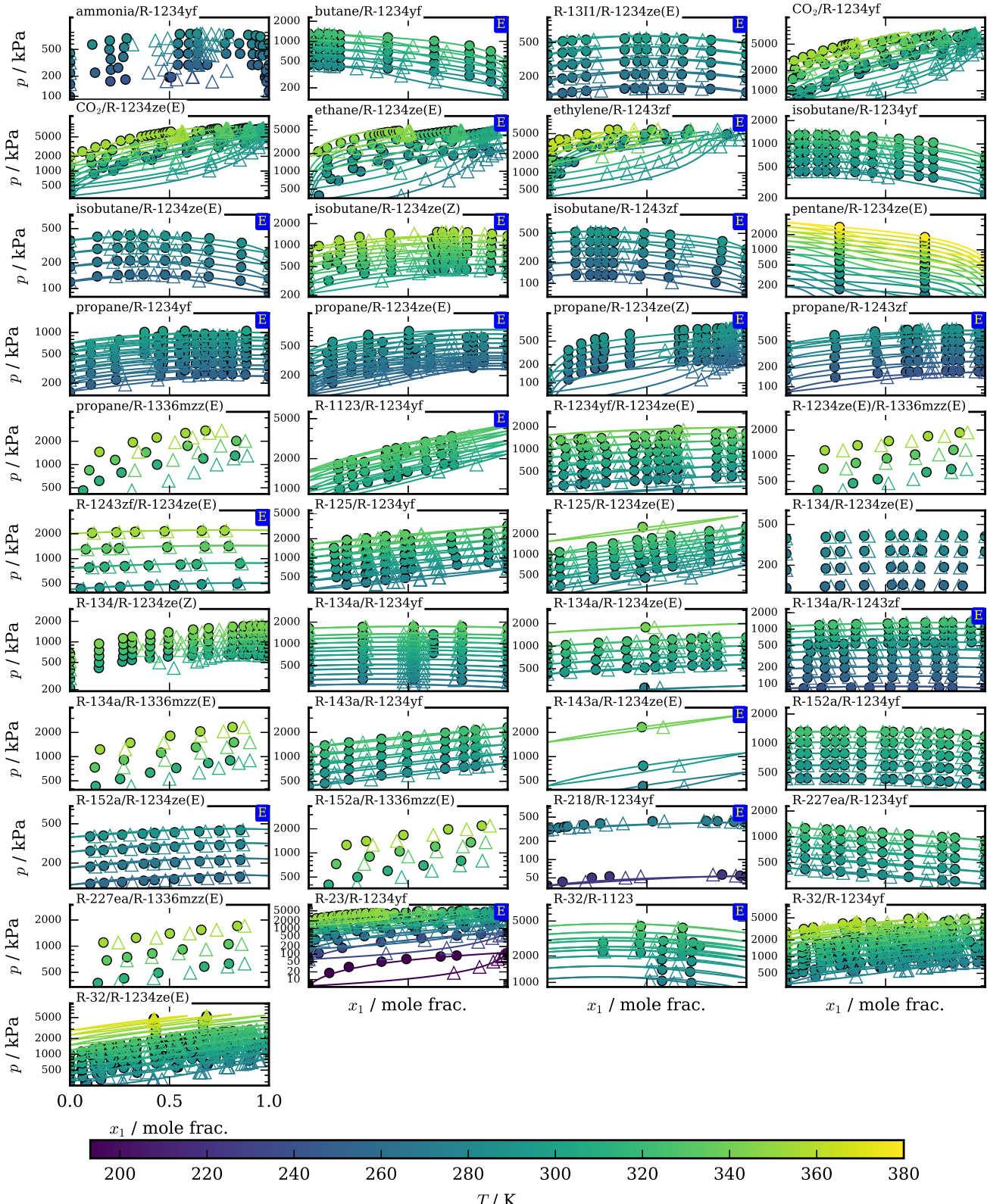


Figure 5: VLE data and models for HFO-containing blends (x_1 is the mole fraction of the first-listed component; E in upper corner: estimated interaction parameters). Larger figures for each binary mixture are in Section 1 of the Supporting Information

deviations are relative to the nearest *nominal* isotherm. Figure 6 shows the deviations in pressure for the binary mixtures considered here. As mentioned above, much of the apparent model fidelity (deviations less than 1%) is a consequence of the experimental data being far below the critical temperatures of the pure fluids. The deviations in pressure for R-32 + R-1234yf (and a number of other fluids) appear large, but much of that is a consequence of the slope of the isotherms going towards infinity in the critical region.

The estimation schemes yield adequate predictions of VLE in some cases, but not universally. The estimation scheme should not have been used for R-13I1 + R-1234ze(E), isobutane + R-1234ze(E), and propane + R-1234ze(E) in REFPROP 10.0; fitted parameters are available in Bell and Lemmon.¹¹⁷ The reason the fitted parameters for mixtures with R-1234ze(E) were erroneously not implemented into REFPROP 10.0 is described in Bell and McLinden.¹²⁰

For a few mixtures, measurements of the critical loci (critical temperature, pressure, and density) are available. In some cases, the critical loci are not directly measured, rather they are extrapolations of measurements at lower pressures. Calculation of the critical curve emanating from a pure component's critical point¹²² or all the critical points for a single composition¹²³ are possible; these two complementary approaches can be used to obtain the full suite of critical curves. Alternatively, the implementation of REFPROP 10.0 obtains the critical points from interpolation of the isopleth of the phase envelope. This method works well for binary refrigerant mixtures, which tend to be Type I in the classification scheme of van Konynenburg and Scott,¹²⁴ although the values obtained are not consistent with the thermodynamic model to numerical precision. As the asymmetry of mixtures increases, a wider range of phase equilibria become possible.¹²⁵

The most reliable critical points are those obtained by tracing the complete critical curve starting at one pure fluid. A complete reimplementation of the mixture model with arbitrary numerical types was carried out, and

is provided in the Supporting Information; a manuscript describing this library is forthcoming. This new generic library allows for calculation of all residual properties by implementing only the residual Helmholtz energy of the model (no error-prone derivatives need to be worked out by hand). The data representation format of CoolProp¹¹⁶ is used, and all required properties can be obtained to numerical precision by complex step derivatives and multicomplex derivatives. The arclength tracing approach for critical loci¹²² is used, with polishing carried out at fixed mixture composition after each simple Euler step of the integration. Figure 7 show results for two mixtures with R-1234yf. The critical loci of the mixture of R-32 + R-1234yf are in qualitative agreement with the experimental data, while the results for CO₂ + R-1234yf correspond to a qualitatively incorrect representation of the critical loci. The remaining binary mixtures are in Section 2 of the Supporting Information. The same critical loci (intermixed with some algorithmic failures) are obtained from the tracing method of Ref. 123 as implemented in CoolProp version 6.4.1.¹¹⁶ The interpolation of the isopleths used in REFPROP 10.0 is also error-prone, and some defects of this approach can be seen in the figures in the Supporting Information. A Python implementation of the critical locus tracing code has also been used in Ref. 126 for non-Type I mixtures containing hydrogen.

3.4 Density

Density data play an important role in thermodynamic model development and the representation of density data (in addition to VLE data) can provide important information regarding the overall quality of a mixture model.

The most comprehensively studied HFO-containing binary mixture is R-32 + R-1234yf. Most of the experimental data are well represented by the model, but a few datasets show large deviations (see Fig. 8). The reasons for these large deviations are explored here, demonstrating that the thermodynamic model is still behaving in a reasonable fashion.

The data from Akasaka et al.⁸⁶ represent sat-

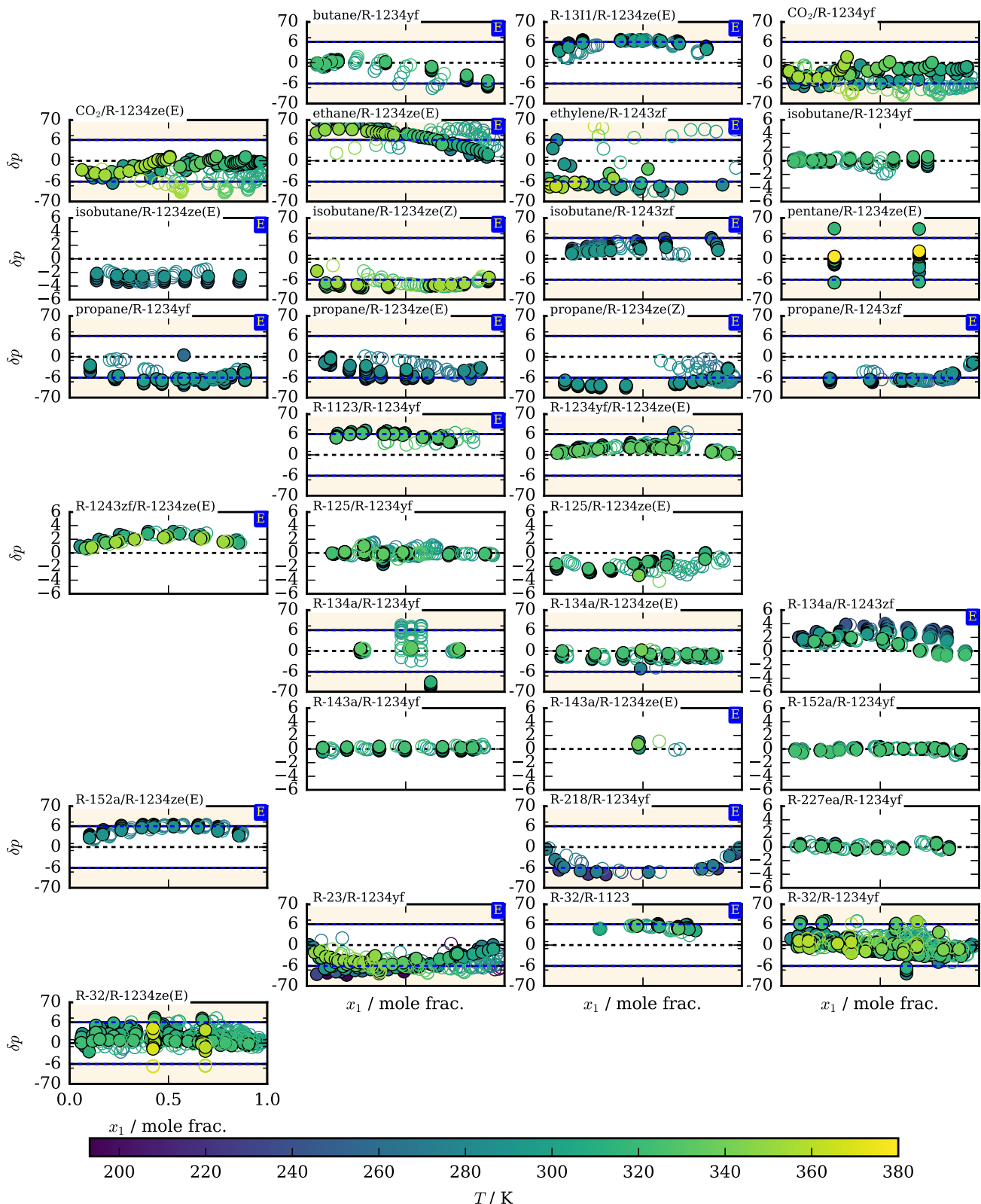


Figure 6: Deviations in pressure ($\delta p \equiv 100 \times (p_{\text{REFPROP}}/p_{\text{exp}} - 1)$) between VLE data points and models for binary mixtures containing halogenated olefins. The ordinates of axes with deviations greater than $\pm 6\%$ are on a logarithmic scale outside $\pm 6\%$, as indicated by a colored fill. The order of the binary pairs on the page follows Fig. 5; mixtures where estimation is not possible or where any component is not in REFPROP 10.0 are not shown, corresponding to the blank areas in the grid. See Fig. 5 for additional information on the figure. Larger figures are available in Section 1 of the Supporting Information

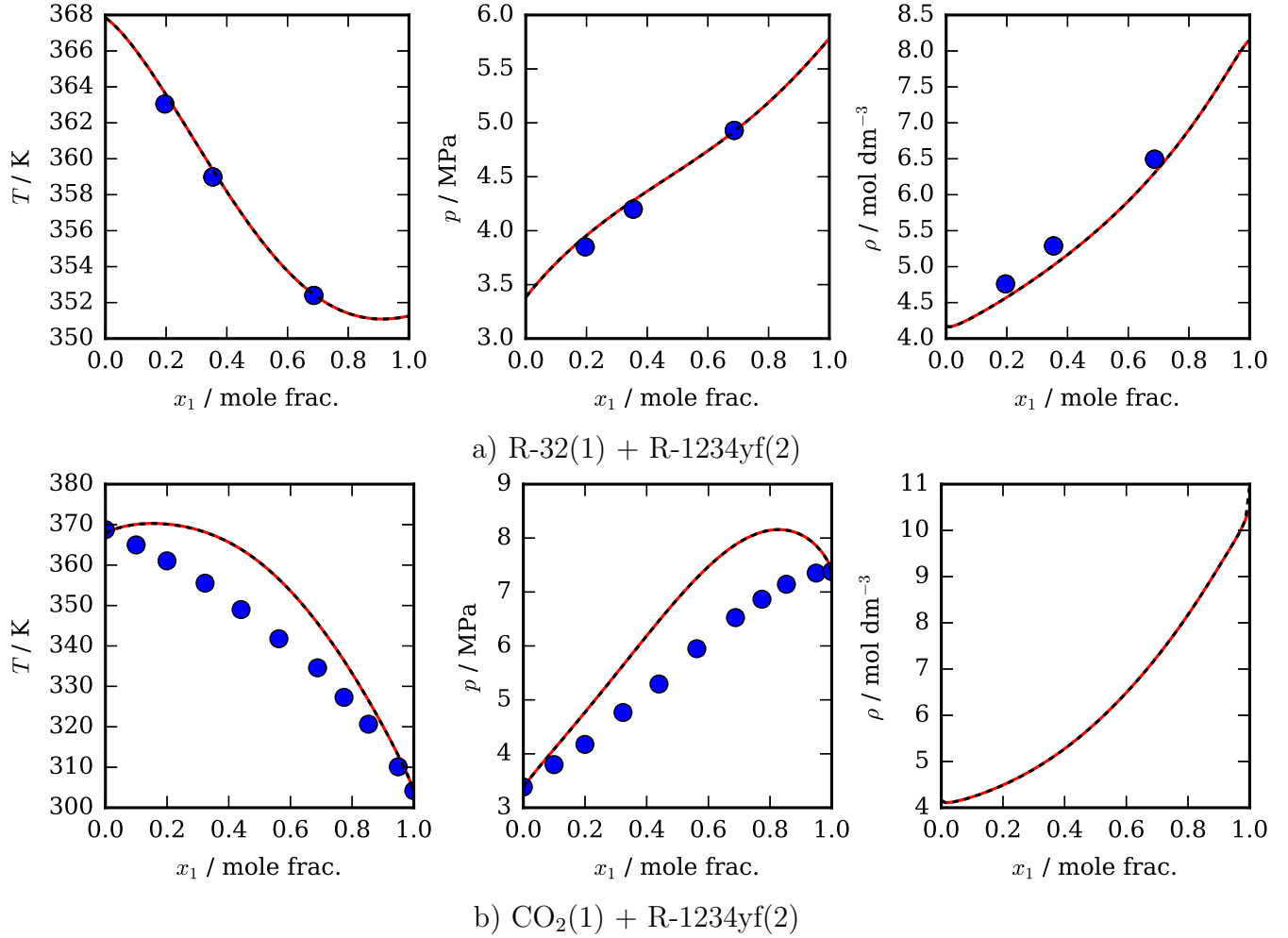


Figure 7: Critical loci for R-32 + R-1234yf and CO₂ + R-1234yf as a function of the mole fraction x_1 . Experimental data^{14,86} are markers, red curves are from the critical curve tracing and dashed black curves are results from REFPROP 10.0 from interpolation of isopleths of the phase envelope.

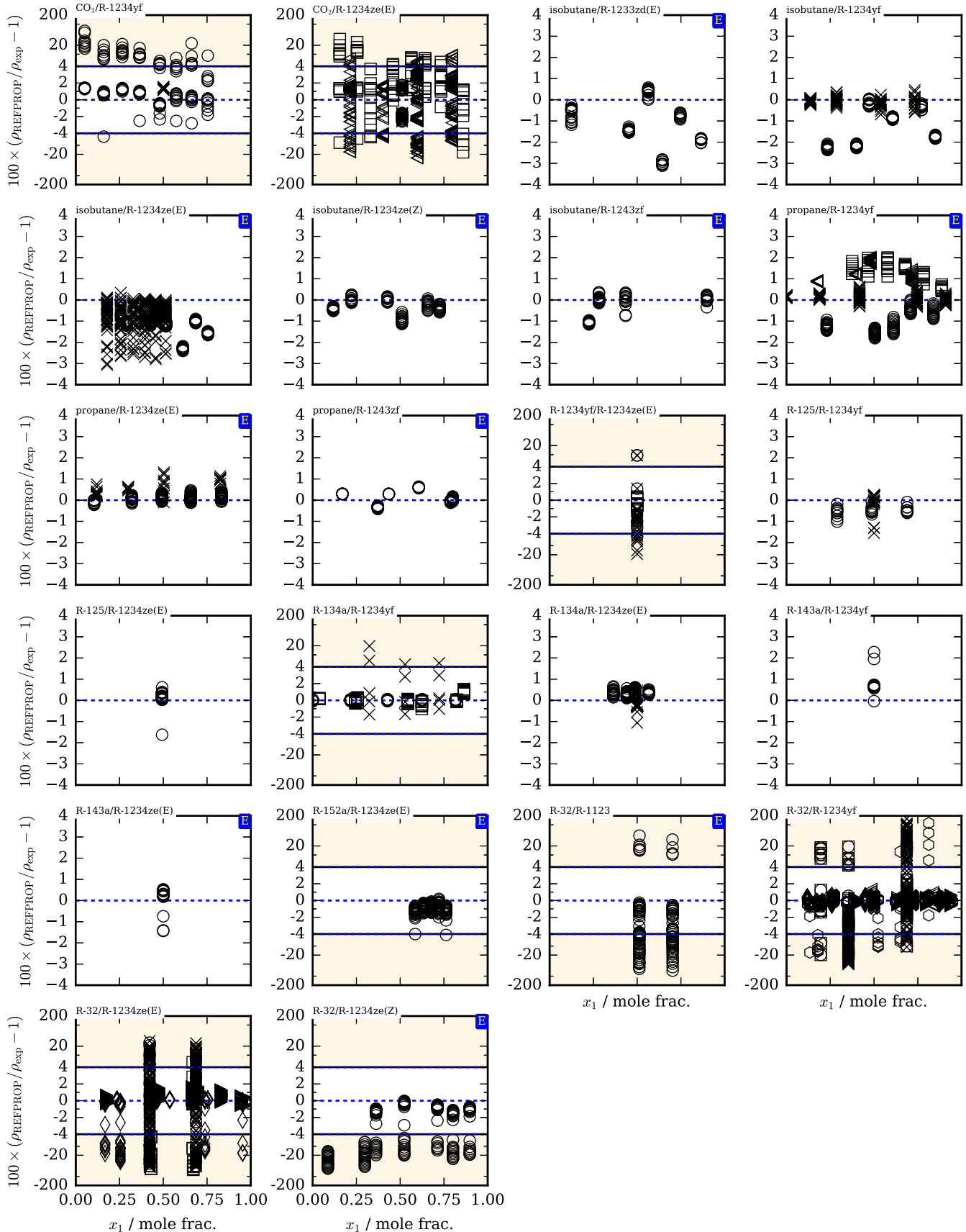


Figure 8: Deviation plots in density for binary mixtures containing halogenated olefins with both components available in REFPROP 10.0¹¹⁵ as a function of x_1 , the mole fraction of the first listed component. The ordinates of axes with deviations greater than $\pm 4\%$ are on a logarithmic scale outside $\pm 4\%$, as indicated by a colored fill. Different plotting symbols indicate different data sources; they are defined in the larger figures in Section 3 in the Supporting Information.

uration phase densities in the critical region, and the model of REFPROP yields deviations in density for these data greater than $\pm 10\%$. A detailed view of these data is available in Fig. 9. While the density deviations may indeed be greater than 10%, much of that deviation is a consequence of the shape of the phase equilibrium curves. The deviations in density represent horizontal shifts in the axis coordinates. The model does not miss the data by much in the temperature direction. The difficulty of assessing model quality for saturated phase density in the critical region mirrors the discussion about VLE deviations described above. The phase equilibrium curve from the model doesn't capture the same asymmetric behavior, skewed to the left (in the figure coordinates).

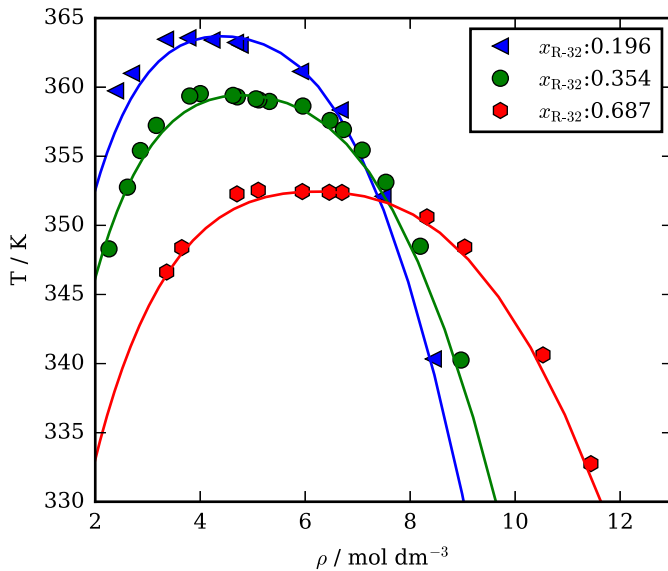


Figure 9: R-32 + R-1234yf equilibrium phase density data from Akasaka et al.⁸⁶ along curves of fixed mole fraction x_{R-32} in the critical region. Solid curves are the isopleths of the phase envelope as obtained from NIST REFPROP 10.0 via CoolProp 6.4.1.¹¹⁶

The second dataset for R-32 + R-1234yf with very large deviations is that of Tomassetti et al.⁹⁰ These data were obtained from quasi-isochoric measurements corresponding to a mixture of constant mass and composition contained in a nearly constant volume chamber, and they extended into the two-phase region. Along each quasi-isochoore, the relationship be-

tween temperature and pressure between the experimental data and the model agree well in a qualitative sense (see Fig. 10). The modeled density in the two-phase region is very sensitive to small errors in the pressure, and thus the deviations in density are artificially high.

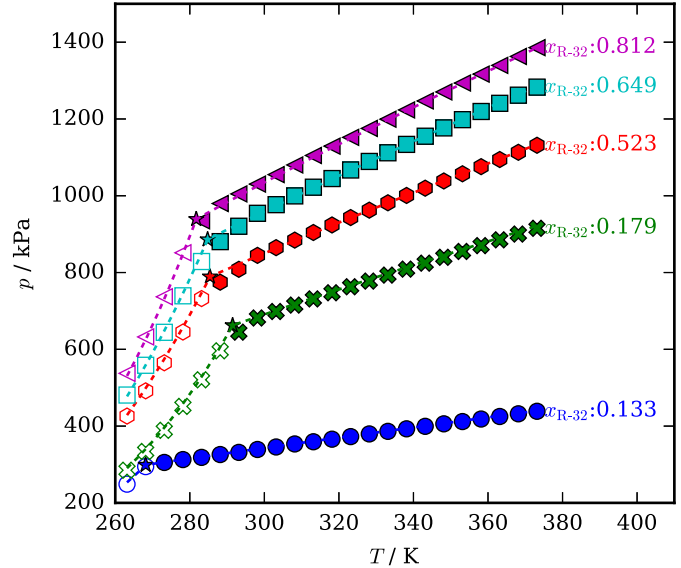


Figure 10: R-32 + R-1234yf quasi-isochoric data from Tomassetti et al.⁹⁰ as a function of temperature and mole fraction for compositions where there are at least one two-phase data-point. Open markers are two-phase data, and filled markers are single-phase, according to the publication. Dashed curves are obtained from NIST REFPROP 10.0; in order to draw the curve the mean composition along each quasi-isochoore of fixed mole fraction composition was used to obtain each pressure for the specified temperature. The stars indicate interpolated dew points from the isopleth of the phase envelope.

After removing the two-phase and near-critical data points described above, the remaining data for the mixture of R-32 + R-1234yf are represented with an absolute average relative difference (AARD) of 0.254 %, as shown in Fig. 11. The near-saturation points (one per composition) from Tomassetti et al.⁹⁰ show evidence of adsorption as indicated by a pressure lower than the extrapolation of the single-phase data, and these points were also dropped.

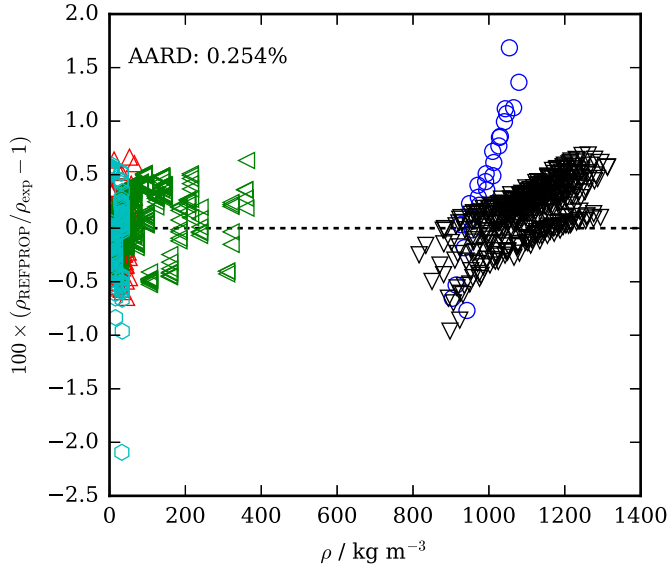


Figure 11: R-32 + R-1234yf density deviations according to experimental data (\circ : Dang et al.,⁷⁸ \triangle : Cai et al.,⁸⁷ \times : Yang et al.,⁸⁸ ∇ : Jia et al.,⁸⁹ \square : Tomassetti et al.⁹⁰) after removing two-phase data and near-critical data.

4 Discussion and Conclusions

The present work surveys the thermodynamic data for blends containing halogenated olefins published in the open literature. While we have almost certainly missed some sources, this is the most comprehensive compilation to date. We included the chlorine-containing HCFOs and HCOs in our search, but found only one dataset for a mixture of R-1233zd(E) + isobutane.

The comparison of these data to the mixture models currently in the NIST REFPROP database show a variety of behaviors. In many cases, the present models represent the available data with an uncertainty adequate for engineering design. In other cases, the deviations between the data and models are large. For mixtures with ammonia, R-134, and R-1336mzz(E) comparisons are not possible because of limitations in the mixture model or missing pure-fluid EOS.

But often, even when the deviations are small, the adjustable parameters in the mixture models have been fitted to only one or two data sets, and often the data extend over a limited range

of temperature and/or composition. Of particular concern is that for many binary pairs only VLE data have been measured. The adequacy of a mixture model intended for refrigeration cycle analysis requiring values for enthalpy, entropy, heat capacity, etc., when that model is fitted only to VLE data, is an open question. Additional density, heat capacity, and speed-of-sound data are needed, especially for mixtures being commercialized. Even for VLE data, confirming data sets are currently available for a limited number of binary pairs, and additional measurements would be very valuable.

Measurements are underway in our group at NIST to fill in some of the data gaps noted here. These include speed-of-sound and density measurements over a wide range of temperature and pressure. We are also aware of work at other institutions around the world carrying out similar measurements. The present literature survey, together with these new data, will form the basis for the development of a mixture model for blends containing halogenated olefins along the lines of the work of Lemmon and Jacobsen¹⁰⁹ for the HFC blends, which has served the refrigeration industry well for nearly two decades.

In summary, this study highlights that there is a need to refit existing models for refrigerant blends. In some cases, the requisite experimental data already exist in the open literature to significantly improve mixture models. In many other cases, additional confirmatory measurements are required from independent research groups in order to ascertain the quality of the existing experimental data.

Supporting Information Available

The Supporting Information includes:

- Larger versions of the figures contained in Fig. 5, Fig. 6, and Fig. 8
- A complete bibliography of the data in Fig. 3 and Fig. 4
- The C++ code used to trace the critical locus

Acknowledgement We gratefully acknowledge the support of the U.S. Department of Energy, Building Technologies Office under Agreement 892434-19-S-EE000031. We also thank Ryo Akasaka (of Kyushu Sangyo University) for help accessing data and literature from Japanese publications.

References

- (1) ASHRAE, ANSI/ASHRAE Standard 34-2019 Designation and Safety Classification of Refrigerants. 2019.
- (2) ISO 817:2014(E) *Refrigerants – Designation and safety classification, Third edition*; Standard, 2014.
- (3) Bell, I. H.; Domanski, P. A.; McLinden, M. O.; Linteris, G. T. The hunt for nonflammable refrigerant blends to replace R-134a. *Int. J. Refrig.* **2019**, *104*, 484–495, DOI: 10.1016/j.ijrefrig.2019.05.035.
- (4) McLinden, M. O.; Brown, J. S.; Brignoli, R.; Kazakov, A. F.; Domanski, P. A. Limited options for low-global-warming-potential refrigerants. *Nat. Commun.* **2017**, *8*, 14476, DOI: 10.1038/ncomms14476.
- (5) ASHRAE, Addendum ac to ANSI/ASHRAE Standard 34-2013 Designation and Safety Classification of Refrigerants. 2013.
- (6) Bobbo, S.; Di Nicola, G.; Zilio, C.; Brown, J. S.; Fedele, L. Low GWP halocarbon refrigerants: A review of thermophysical properties. *Int. J. Refrig.* **2018**, *90*, 181–201, DOI: 10.1016/j.ijrefrig.2018.03.027.
- (7) Kayukawa, Y.; Sakoda, N.; Akasaka, R. A Review on Thermophysical Property Researches for Low-GWP Olefin Refrigerants. *Trans. of the JSRAE*. 2020; pp 1–44.
- (8) Nair, V. HFO refrigerants: A review of present status and future prospects. *Int. J. Refrig.* **2021**, *122*, 156–170, DOI: 10.1016/j.ijrefrig.2020.10.039.
- (9) Hashimoto, M.; Otsuka, T.; Fukushima, M.; Okamoto, H.; Hayamizu, H.; Ueno, K.; Akasaka, R. Development of New Low-GWP Refrigerants-Refrigerant Mixtures Including HFO-1123. *Sci. Technol. Built Environ.* **2019**, *25*, 776–783, DOI: 10.1080/23744731.2019.1603779.
- (10) Hanwell, M. D.; Curtis, D. E.; Lonie, D. C.; Vandermeersch, T.; Zurek, E.; Hutchison, G. R. Avogadro: an advanced semantic chemical editor, visualization, and analysis platform. *J. Cheminform.* **2012**, *4*, 17, DOI: 10.1186/1758-2946-4-17.
- (11) Zhao, Y.; Dong, X.; Zhong, Q.; Li, H.; Zhang, H.; Gong, M.; Shen, J. The experimental investigation of the vapour liquid phase equilibrium for (ammonia + 2,3,3,3-tetrafluoroprop-1-ene) system. *J. Chem. Thermodyn.* **2017**, *113*, 257–262, DOI: 10.1016/j.jct.2017.06.018.
- (12) Hu, P.; Zhang, N.; Chen, L.-X.; Cai, X.-D. Vapor-Liquid Equilibrium Measurements for 2,3,3,3-Tetrafluoroprop-1-ene + Butane at Temperatures from 283.15 to 323.15 K. *J. Chem. Eng. Data* **2018**, *63*, 1507–1512, DOI: 10.1021/acs.jced.7b01073.
- (13) Guo, H.; Gong, M.; Dong, X.; Wu, J. (Vapour + liquid) equilibrium data for the binary system of (trifluoroiodomethane (R13I1) + trans-1, 3, 3, 3-tetrafluoropropene (R1234ze (E))) at various temperatures from (258.150 to 298.150) K. *J. Chem. Thermodyn.* **2012**, *47*, 397–401, DOI: 10.1016/j.jct.2011.11.024.
- (14) Juntarachat, N.; Valtz, A.; Coquelet, C.; Privat, R.; Jaubert, J.-N. Experimental measurements and correlation of

- vapor-liquid equilibrium and critical data for the CO₂ + R1234yf and CO₂ + R1234ze(E) binary mixtures. *Int. J. Refrig.* **2014**, *47*, 141–152, DOI: 10.1016/j.ijrefrig.2014.09.001.
- (15) Arami-Niya, A.; Xiao, X.; Al Ghafri, S. Z.; Jiao, F.; Khamphasith, M.; Pouya, E. S.; Sadaghiani, M. S.; Yang, X.; Tsuji, T.; Tanaka, Y.; Seiki, Y.; May, E. F. Measurement and modelling of the thermodynamic properties of carbon dioxide mixtures with HFO-1234yf, HFC-125, HFC-134a, and HFC-32: vapour-liquid equilibrium, density, and heat capacity. *Int. J. Refrig.* **2020**, *118*, 514–528, DOI: 10.1016/j.ijrefrig.2020.05.009.
- (16) Wang, S.; Fauve, R.; Coquelet, C.; Valtz, A.; Houriez, C.; Artola, P.-A.; El Ahmar, E.; Rousseau, B.; Hu, H. Vapor liquid equilibrium and molecular simulation data for carbon dioxide (CO₂) + trans-1,3,3,3-tetrafluoroprop-1-ene (R-1234ze(E)) mixture at temperatures from 283.32 to 353.02 K and pressures up to 7.6 MPa. *Int. J. Refrig.* **2019**, *98*, 362–371, DOI: 10.1016/j.ijrefrig.2018.10.032.
- (17) Liu, Y.; Valtz, A.; Abbadi, J. E.; He, G.; Coquelet, C. Isothermal Vapor-Liquid Equilibrium Measurements for the (R1234ze(E) + Ethane) System at Temperatures from 272.27 to 347.52 K. *J. Chem. Eng. Data* **2018**, *63*, 4185–4192, DOI: 10.1021/acs.jced.8b00653.
- (18) Zernov, V. S.; Kogan, V. B.; Lyubetskii, S. G.; Duntov, F. I. Liquid-vapor equilibrium in the system ethylene + trifluoropropylene. *Zh. Prikl. Khim.* **1971**, *44*, 683–686.
- (19) Hu, P.; Chen, L.-X.; Chen, Z. Vapor-liquid equilibria for binary system of 2,3,3,3-tetrafluoroprop-1-ene (HFO-1234yf) + isobutane (HC-600a). *Fluid Phase Equilibr.* **2014**, *365*, 1–4, DOI: 10.1016/j.fluid.2013.12.015.
- (20) Dong, X.; Gong, M.; Shen, J.; Wu, J. Vapor Liquid Equilibria of the trans-1,3,3,3-Tetrafluoropropene (R1234ze(E)) + Isobutane (R600a) System at Various Temperatures from (258.150 to 288.150) K. *J. Chem. Eng. Data* **2012**, *57*, 541–544, DOI: 10.1021/je2011055.
- (21) Zhang, X.; Dong, X.; Guo, H.; Gong, M.; Shen, J.; Wu, J. Measurements and correlations of isothermal (vapour + liquid) equilibrium for the (isobutane (R600a) + cis-1,3,3,3-tetrafluoropropene (R1234ze(Z))) system at temperatures from (303.150 to 353.150) K. *J. Chem. Thermodyn.* **2016**, *103*, 349–354, DOI: 10.1016/j.jct.2016.08.031.
- (22) Deng, Z.; Xu, G.; Sun, S.; Zhao, Y.; Dong, X.; Gong, M. Isothermal (vapour-liquid) equilibrium for the binary (isobutane (R600a) + 3,3,3-trifluoropropene (R1243zf)) system at temperatures from 253.150 to 293.150 K. *J. Chem. Thermodyn.* **2020**, *150*, 106177, DOI: 10.1016/j.jct.2020.106177.
- (23) Outcalt, S. L.; Lemmon, E. W. Bubble-Point Measurements of Eight Binary Mixtures for Organic Rankine Cycle Applications. *J. Chem. Eng. Data* **2013**, *58*, 1853–1860, DOI: 10.1021/je400251s.
- (24) Zhong, Q.; Dong, X.; Zhao, Y.; Li, H.; Zhang, H.; Guo, H.; Gong, M. Measurements of isothermal vapour liquid equilibrium for the 2,3,3,3-tetrafluoroprop-1-ene + propane system at temperatures from 253.150 to 293.150 K. *Int. J. Refrig.* **2017**, *81*, 26–32, DOI: 10.1016/j.ijrefrig.2017.05.016.
- (25) Zhong, Q.; Li, H.; Dong, X.; Zhang, H.; Zhao, Y.; Guo, H.; Shen, J.; Gong, M. Measurements of bubble point pressure and saturated liquid density for ((R1234yf + R290)). *J. Chem. Thermodyn.* **2018**, *118*, 77–81, DOI: 10.1016/j.jct.2017.10.016.

- (26) Dong, X.; Gong, M.; Shen, J.; Wu, J. Experimental measurement of vapor-liquid equilibrium for (trans-1,3,3,3-tetrafluoropropene (R1234ze(E)) + propane (R290)). *Int. J. Refrig.* **2011**, *34*, 1238–1243, DOI: 10.1016/j.ijrefrig.2011.03.007.
- (27) Zhang, H.; Zhong, Q.; Gong, M.; Li, H.; Dong, X.; Shen, J.; Wu, J. Experimental Study on the Saturated Liquid Density and Bubble Point Pressure for R1234ze(E) + R290. *J. Chem. Eng. Data* **2016**, *61*, 3241–3249, DOI: 10.1021/acs.jced.6b00327.
- (28) Gong, M.; Zhao, Y.; Dong, X.; Guo, H.; Shen, J.; Wu, J. Measurements of isothermal (vapor + liquid) equilibrium for the (propane + cis-1,3,3,3-tetrafluoropropene) system at temperatures from (253.150 to 293.150) K. *J. Chem. Thermodyn.* **2016**, *98*, 319–323, DOI: 10.1016/j.jct.2016.03.018.
- (29) Ding, L.; Yao, X.; Hou, Y.; Zhao, Y.; Dong, X.; Gong, M. Isothermal (vapour-liquid) equilibrium for the binary (3,3,3-trifluoropropene (R1243zf) + propane(R290)) system at temperatures from 243.150 K to 288.150 K. *J. Chem. Thermodyn.* **2020**, *144*, 106091, DOI: 10.1016/j.jct.2020.106091.
- (30) Boonaert, E.; Valtz, A.; Brocuss, J.; Coquelet, C.; Beucher, Y.; De Carlan, F.; Fourmigue, J.-M. Vapor-liquid equilibrium measurements for 5 binary mixtures involving HFO-1336mzz(E) at temperatures from 313 to 353 K and pressures up to 2.735 MPa. *Int. J. Refrig.* **2020**, *114*, 210–220, DOI: 10.1016/j.ijrefrig.2020.02.016.
- (31) Miyamoto, H.; Nishida, M.; Saito, T. Measurement of the vapour-liquid equilibrium properties of binary mixtures of the low-GWP refrigerants R1123 and R1234yf. *J. Chem. Thermodyn.* **2021**, *158*, 106456, DOI: 10.1016/j.jct.2021.106456.
- (32) Al Ghafri, S. Z.; Rowland, D.; Akhfash, M.; Arami-Niya, A.; Khamphasith, M.; Xiao, X.; Tsuji, T.; Tanaka, Y.; Seiki, Y.; May, E. F.; Hughes, T. J. Thermodynamic properties of hydrofluoroolefin (R1234yf and R1234ze(E)) refrigerant mixtures: Density, vapour-liquid equilibrium, and heat capacity data and modelling. *Int. J. Refrig.* **2019**, *98*, 249–260, DOI: 10.1016/j.ijrefrig.2018.10.027.
- (33) Ye, G.; Fang, Y.; Guo, Z.; Ni, H.; Zhuang, Y.; Han, X.; Chen, G. Experimental Investigation of Vapor Liquid Equilibrium for 2,3,3,3-Tetrafluoropropene (HFO-1234yf)+trans-1,3,3,3-Tetrafluoropropene (HFO-1234ze(E)) at Temperatures from 284 to 334 K. *J. Chem. Eng. Data* **2021**, *66*, 1741–1753.
- (34) Yang, Z.; Valtz, A.; Coquelet, C.; Wu, J.; Lu, J. Experimental measurement and modelling of vapor-liquid equilibrium for 3,3,3-Trifluoropropene (R1243zf) and trans-1,3,3,3-Tetrafluoropropene (R1234ze(E)) binary system. *Int. J. Refrig.* **2020**, *120*, 137–149, DOI: 10.1016/j.ijrefrig.2020.08.016.
- (35) Kamiaka, T.; Dang, C.; Hihara, E. Vapor-Liquid Equilibrium Measurements of HFC-32+HFO-1234yf and HFC-125+HFO-1234yf Refrigerant Mixture. JSRAE Annual Conference. Kanazawa, 2010.
- (36) Kamiaka, T.; Dang, C.; Hihara, E. Vapor-liquid equilibrium measurements for binary mixtures of R1234yf with R32, R125, and R134a. *Int. J. Refrig.* **2013**, *36*, 965–971, DOI: 10.1016/j.ijrefrig.2012.08.016.
- (37) Yang, T.; Hu, X.; Meng, X.; Wu, J. Vapour-liquid equilibria for the binary systems of pentafluoroethane ((R125) + 2,3,3,3-tetrafluoroprop-1-ene (R1234yf)) and (trans-1,3,3,3-tetrafluoropropene R1234ze(E)). *J.*

- Chem. Thermodyn.* **2020**, *150*, 106222, DOI: 10.1016/j.jct.2020.106222.
- (38) Dong, X.; Guo, H.; Gong, M.; Yang, Z.; Wu, J. Measurements of isothermal (vapour + liquid) equilibria data for (1,1,2,2-Tetrafluoroethane (R134) + trans-1,3,3,3-tetrafluoropropene (R1234ze (E))) at T = (258.150 to 288.150) K. *J. Chem. Thermodyn.* **2013**, *60*, 25–28, DOI: 10.1016/j.jct.2012.12.026.
- (39) Zhang, X.; Dong, X.; Guo, H.; Zhao, Y.; Zhang, H.; Gong, M.; Shen, J. Measurements of isothermal (vapour + liquid) equilibrium for the 1,1,2,2-1,1,2,2-tetrafluoroethane (R134) + cis-1,3,3,3-tetrafluoropropene (R1234ze(Z)) system at temperatures from (303.150 to 343.150) K. *J. Chem. Thermodyn.* **2017**, *111*, 20–26, DOI: 10.1016/j.jct.2017.03.010.
- (40) Shimoura, H.; Matsuo, S.; Sotani, T. Speed of sound measurements in dense liquid of low GWP refrigerant mixture including HFO-1234yf. The 32nd Japan Symposium on Thermophysical Properties. Yokohama: Japan, 2011.
- (41) Chen, R.; Qi, Y.; Wu, D. Experimental Study of PVTx Properties of Mixture Refrigerant R1234yf/R134a. *Zhileng Xuebao* **2016**, *37*, 18–25, DOI: 10.3969/j.issn.0253-4339.2016.01.018.
- (42) Kou, L.; Yang, Z.; Tang, X.; Zhang, W.; Lu, J. Experimental measurements and correlation of isothermal vapor-liquid equilibria for HFC-32 + HFO-1234ze (E) and HFC-134a + HFO-1234ze (E) binary systems. *J. Chem. Thermodyn.* **2019**, *139*, 105798, DOI: 10.1016/j.jct.2019.04.020.
- (43) Yang, Z.; Tang, X.; Wu, J.; Lu, J. Experimental measurements of saturated vapor pressure and isothermal vapor-liquid equilibria for 1,1,1,2-Tetrafluoroethane (HFC-134a) + 3,3,3-trifluoropropene (HFO-1243zf) binary system. *Fluid Phase Equilib.* **2019**, *498*, 86–93, DOI: 10.1016/j.fluid.2019.06.020.
- (44) Yao, X.; Ding, L.; Dong, X.; Zhao, Y.; Wang, X.; Shen, J.; Gong, M. Experimental measurement of vapor-liquid equilibrium for 3,3,3-trifluoropropene (R1243zf) + 1,1,1,2-tetrafluoroethane (R134a) at temperatures from 243.150 to 293.150 K. *Int. J. Refrig.* **2020**, *120*, 97–103, DOI: 10.1016/j.ijrefrig.2020.09.008.
- (45) Hu, P.; Chen, L.-X.; Chen, Z. Vapor-liquid equilibria for the 1,1,1,2 -tetrafluoroethane (HFC-134a) + 1,1,1,2,3,3,3-heptafluoropropane (HFC-227ea) and 1,1,1-trifluoroethane (HFC-143a) + 2,3,3,3-tetrafluoroprop-1-ene (HFO-1234yf) systems. *Fluid Phase Equilib.* **2013**, *360*, 293–297, DOI: 10.1016/j.fluid.2013.09.056.
- (46) Hu, P.; Chen, L.-X.; Zhu, W.-B.; Jia, L.; Chen, Z. Isothermal VLE measurements for the binary mixture of 2,3,3,3-tetrafluoroprop-1-ene (HFO-1234yf) + 1,1-difluoroethane (HFC-152a). *Fluid Phase Equilib.* **2014**, *373*, 80–83, DOI: 10.1016/j.fluid.2014.04.015.
- (47) Yang, T.; Hu, X.; Meng, X.; Wu, J. Vapor-Liquid Equilibria for the Binary and Ternary Systems of Difluoromethane (R32), 1,1-Difluoroethane (R152a), and 2,3,3,3-Tetrafluoroprop-1-ene (R1234yf). *J. Chem. Eng. Data* **2018**, *63*, 771–780, DOI: 10.1021/acs.jced.7b00950.
- (48) Yang, Z.; Gong, M.; Guo, H.; Dong, X.; Wu, J. Phase equilibrium for the binary mixture of (1,1-difluoroethane (R152a) + trans-1,3,3,3-tetrafluoropropene (R1234ze (E))) at various temperatures from 258.150 to 288.150 K. *Fluid Phase Equilib.* **2013**, *355*, 99–103, DOI: 10.1016/j.fluid.2013.06.017.

- (49) Kochenburger, T. M.; Gomse, D.; Tratschitt, I.; Zimmermann, A.; Grohmann, S. Vapor-liquid and vapor-liquid-liquid equilibrium measurements and correlation of the binary mixtures 2,3,3,3-tetrafluoroprop-1-ene (R1234yf) + (tetrafluoromethane (R14), trifluoromethane (R23), octafluoropropane (R218), nitrogen (R728) and argon (R740)) and ethane (R170) + trifluoromethane (R23). *Fluid Phase Equilib.* **2017**, *450*, 13–23, DOI: 10.1016/j.fluid.2017.07.002.
- (50) Hu, P.; Chen, L.-X.; Zhu, W.-B.; Jia, L.; Chen, Z. Vapor-liquid equilibria for the binary system of 2,3,3,3-tetrafluoroprop-1-ene (HFO-1234yf) + 1,1,1,2,3,3,3-heptafluoropropane (HFC-227ea)). *Fluid Phase Equilib.* **2014**, *379*, 59–61, DOI: 10.1016/j.fluid.2014.07.014.
- (51) Madani, H.; Valtz, A.; Zhang, F.; Abbadi, J. E.; Houriez, C.; Paricaud, P.; Coquelet, C. Isothermal vapor-liquid equilibrium data for the trifluoromethane (R23) + 2,3,3,3-tetrafluoroprop-1-ene (R1234yf) system at temperatures from 254 to 348 K. *Fluid Phase Equilib.* **2016**, *415*, 158–165, DOI: 10.1016/j.fluid.2016.02.005.
- (52) Miyamoto, H.; Saito, T.; Sakoda, N.; Perera, U.; Ishii, T.; Thu, K.; Higashi, Y. Measurement of the vapor-liquid equilibrium properties of the binary low GWP refrigerant R32/R1123. *Int. J. Refrig.* **2020**, *119*, 340–348, DOI: 10.1016/j.ijrefrig.2020.07.005.
- (53) Kobayashi, K.; Tanaka, K.; Higashi, Y. Measurements of $P\rho Tx$ Properties for the Binary HFO-1234yf + HFC-32 Mixtures. International Congress of Refrigeration. Prague: Czech Republic, 2011.
- (54) Hu, X.; Yang, T.; Meng, X.; Bi, S.; Wu, J. Vapor liquid equilibrium measurements for difluoromethane (R32) + 2,3,3,3-tetrafluoroprop-1-ene (R1234yf) and fluoroethane (R161) + 2,3,3,3-tetrafluoroprop-1-ene (R1234yf). *Fluid Phase Equilib.* **2017**, *438*, 10–17, DOI: 10.1016/j.fluid.2017.01.024.
- (55) Yamada, T.; Miyamoto, H.; Sakoda, N.; Higashi, Y. Vapor-Liquid Equilibrium Property Measurements for R32/R1234yf Binary Mixtures in Low R32 Concentration. *Int. J. Thermophys.* **2020**, *41*, 167, DOI: 10.1007/s10765-020-02752-2.
- (56) Li, S.; Peng, S.; Yang, Z.; Duan, Y. Measurements and correlation of vapor-liquid equilibrium for difluoromethane (R-32) + 2,3,3,3-tetrafluoroprop-1-ene (R-1234yf) and pentafluoroethane (R-125) + propane (R-290). *Fluid Phase Equilib.* **2021**, *538*, 113010, DOI: 10.1016/j.fluid.2021.113010.
- (57) Kobayashi, K.; Tanaka, K.; Higashi, Y. $P\rho Tx$ Property Measurements of Binary HFO-1234ze(E) + HFC-32 Refrigerant Mixtures. *Nippon Reito Kucho Gakkai Ronbunshu* **2011**, *28*, 415–426, DOI: 10.11322/tjsrae.28.415.
- (58) Tanaka, K.; Akasaka, R.; Higashi, Y. Measurements of Density and Isobaric Specific Heat Capacity for HFO-1234ze(E)+HFC-32 Mixtures. *Nippon Reito Kucho Gakkai Ronbunshu* **2011**, *28*, 427–434, DOI: 10.11322/tjsrae.28.427.
- (59) Akasaka, R. Thermodynamic property models for the difluoromethane (R-32) + trans-1,3,3,3-tetrafluoropropene (R-1234ze(E)) and difluoromethane + 2,3,3,3-tetrafluoropropene (R-1234yf) mixtures. *Fluid Phase Equilib.* **2013**, *358*, 98–104, DOI: 10.1016/j.fluid.2013.07.057.
- (60) Hu, X.; Meng, X.; Wu, J. Isothermal vapor liquid equilibrium measurements for difluoromethane (R32) + trans-1,3,3,3-tetrafluoropropene (R1234ze(E)). *Fluid*

- Phase Equilib.* **2017**, *431*, 58–65, DOI: 10.1016/j.fluid.2016.10.011.
- (61) Di Nicola, G.; Di Nicola, C.; Arteconi, A.; Stryjek, R. PVTx Measurements of the Carbon Dioxide + 2,3,3,3-Tetrafluoroprop-1-ene Binary System. *J. Chem. Eng. Data* **2012**, *57*, 450–455, DOI: 10.1021/je201051q.
- (62) Yamaya, K.; Ishiduka, S.; Matsuguchi, A.; Kagawa, N.; Koyama, S. Isochoric Heat Capacity of HFO-1234ze(E) and CO₂ + HFO-1234ze(E) Mixtures in the Liquid Phase. JSRAE Annual Conference. Kanazawa, 2010.
- (63) Yamaya, K.; Matsuguchi, A.; Kagawa, N.; Koyama, S. Isochoric Specific Heat Capacity of trans-1,3,3,3-Tetrafluoropropene (HFO-1234ze(E)) and the HFO-1234ze(E) + CO₂ Mixture in the Liquid Phase. *J. Chem. Eng. Data* **2011**, *56*, 1535–1539, DOI: 10.1021/je101209e.
- (64) Di Nicola, G.; Passerini, G.; Polonara, F.; Stryjek, R. PVTx measurements of the carbon dioxide + trans-1,3,3,3-tetrafluoroprop-1-ene binary system. *Fluid Phase Equilib.* **2013**, *360*, 124–128, DOI: 10.1016/j.fluid.2013.09.022.
- (65) Fu, Y.; Valtz, A.; Ahamada, S.; Hu, H.; Coquelet, C. Density data for carbon dioxide (CO₂) +trans-1,3,3,3-tetrafluoroprop-1-ene (R-1234ze(E)) mixture at temperatures from 283.32 to 353.02 K and pressures up to 10 MPa. *Int. J. Refrig.* **2020**, *120*, 430–444, DOI: 10.1016/j.ijrefrig.2020.06.006.
- (66) Brown, J. S.; Coccia, G.; Tomassetti, S.; Pierantozzi, M.; Di Nicola, G. Vapor Phase PvTx Measurements of Binary Blends of trans-1-Chloro-3,3,3-trifluoroprop-1-ene + Isobutane and cis-1,3,3,3-Tetrafluoroprop-1-ene + Isobutane. *J. Chem. Eng. Data* **2018**, *63*, 169–177, DOI: 10.1021/acs.jced.7b00769.
- (67) Brown, J. S.; Coccia, G.; Tomassetti, S.; Pierantozzi, M.; Di Nicola, G. Vapor Phase PTx Measurements of Binary Blends of 2,3,3,3-Tetrafluoroprop-1-ene + Isobutane and trans-1,3,3,3-Tetrafluoroprop-1-ene + Isobutane. *J. Chem. Eng. Data* **2017**, *62*, 3577–3584, DOI: 10.1021/acs.jced.7b00564.
- (68) Zhang, H.; Li, H.; Gao, B.; Zhong, Q.; Wu, W.; Liu, W.; Dong, X.; Gong, M.; Luo, E. Gaseous densities of 2,3,3,3-tetrafluoroprop-1-ene (R1234yf) and isobutane (R600a) binary system: Measurements and a preliminary Helmholtz equation of state. *Int. J. Refrig.* **2018**, *95*, 28–37, DOI: 10.1016/j.ijrefrig.2018.07.029.
- (69) Cao, R.; Qi, Y.; Chen, R. pVTx properties of binary R1234ze(E)/R600a system. *J. Chem. Thermodyn.* **2017**, *111*, 191–198, DOI: 10.1016/j.jct.2017.03.032.
- (70) Tomassetti, S.; Pierantozzi, M.; Di Nicola, G.; Polonara, F.; Brown, J. S. Vapor-Phase PvTx Measurements of Binary Blends of cis-1,2,3,3,3-Pentafluoroprop-1-ene + Isobutane and 3,3,3-Trifluoropropene + Isobutane. *J. Chem. Eng. Data* **2019**, *64*, 688–695, DOI: 10.1021/acs.jced.8b00921.
- (71) Brown, J. S.; Coccia, G.; Di Nicola, G.; Pierantozzi, M.; Polonara, F. Vapor Phase PvTx Measurements of Binary Blends of 2,3,3,3-Tetrafluoroprop-1-ene + Propane and cis-1,2,3,3,3-Pentafluoroprop-1-ene + Propane. *J. Chem. Eng. Data* **2016**, *61*, 3346–3354, DOI: 10.1021/acs.jced.6b00396.
- (72) Zhong, Q.; Dong, X.; Zhang, H.; Li, H.; Gong, M.; Shen, J.; Wu, J. Experimental study on the gaseous pρTx properties for (HFO1234yf + HC290). *J. Chem. Thermodyn.* **2017**, *107*, 126–132, DOI: 10.1016/j.jct.2016.12.029.

- (73) Zhong, Q.; Dong, X.; Zhao, Y.; Zhang, H.; Wang, J.; Guo, H.; Shen, J.; Gong, M. Thermodynamic properties of (R1234yf + R290): Isochoric $p\rho Tx$ and specific heat capacity c_v measurements and an equation of state. *J. Chem. Thermodyn.* **2019**, *129*, 36–43, DOI: 10.1016/j.jct.2018.09.009.
- (74) Zhang, H.; Gong, M.; Li, H.; Guo, H.; Dong, X.; Wu, J. Gaseous $p\rho Tx$ properties for binary mixtures of HFO1234ze(E) + HC290. *Fluid Phase Equilib.* **2016**, *408*, 232–239, DOI: 10.1016/j.fluid.2015.09.010.
- (75) Sheng, B.; Dong, X.; Zhao, Y.; Li, Z.; Yan, H.; Zhong, Q.; Wang, J.; Gong, M.; Shen, J. Measurements of $p\rho Tx$ and specific heat capacity c_V for (R290 + R1243zf) binary mixtures at temperatures from (292 to 350) K and pressures up to 11 MPa. *Int. J. Refrig.* **2020**, *112*, 74–81, DOI: 10.1016/j.ijrefrig.2019.12.030.
- (76) Higashi, Y. Thermophysical Property Measurements for R1234yf + R1234ze(E) Mixture. International Congress of Refrigeration. Yokohama: Japan, 2015.
- (77) Higashi, Y. Measurements of thermodynamic properties for the 50 mass% R1234yf + 50 mass% R1234ze(E) blend. *Sci. Technol. Built Environ.* **2016**, *22*, 1185–1190, DOI: 10.1080/23744731.2016.1223975.
- (78) Dang, Y.; Kamiaka, T.; Dang, C.; Hihara, E. Liquid viscosity of low-GWP refrigerant mixtures (R32 + R1234yf) and (R125 + R1234yf). *J. Chem. Thermodyn.* **2015**, *89*, 183–188, DOI: 10.1016/j.jct.2015.05.009.
- (79) Yotsumoto, Y.; Sugitani, R.; Matsuo, S.; Sotani, T. Density Measurements of Binary Mixtures for (HFO-1234yf + HFC-134a) System. The 31st Japan Symposium on Thermophysical Properties. Fukuoka: Japan, 2010.
- (80) Akasaka, R.; Higashi, Y.; Yamada, Y.; Shibanuma, T. Thermodynamic properties of 1,1,1,2-tetrafluoroethane (R-134a) + 2,3,3,3-tetrafluoropropene (R-1234yf) mixtures: Measurements of the critical parameters and a mixture model based on the multi-fluid approximation. *Int. J. Refrig.* **2015**, *58*, 146–153, DOI: 10.1016/j.ijrefrig.2015.06.011.
- (81) Chen, Q.; Qi, H.; Zhang, S.; Hong, R.; Chen, G. An experimental study of PVTx properties in the gas phase for binary mixtures of HFO-1234yf and HFC-134a. *Fluid Phase Equilib.* **2015**, *385*, 25–28, DOI: 10.1016/j.fluid.2014.10.047.
- (82) Zhang, H.; Dong, X.; Zhong, Q.; Li, H.; Gong, M.; Shen, J.; Wu, J. Investigation of $p\rho Tx$ properties for R1234ze(E) + R134a mixtures in the gas phase. *Int. J. Refrig.* **2017**, *73*, 144–153, DOI: 10.1016/j.ijrefrig.2016.08.016.
- (83) Qi, Y.; Zhang, F.; Nie, Y.; Yang, H.; Zhang, H.; Wu, W. Experimental Study on the PVTx Properties of the R1234ze(E)/R152a System by the Burnett Method. *J. Chem. Eng. Data* **2020**, *65*, 4194–4200, DOI: 10.1021/acs.jced.9b01056.
- (84) Higashi, Y.; Akasaka, R. Measurements of Thermodynamic Properties for R1123 and R1123+R32 Mixture. 16th International Refrigeration and Air Conditioning Conference. Purdue, July 11-July 14, 2016.
- (85) Akatsu, M.; Tanaka, K.; Higashi, Y. Measurements of Saturated Densities and Critical Parameters for the Binary HFO-1234YF + HFC-32 Mixtures. International Congress of Refrigeration. Prague: Czech Republic, 2011.
- (86) Akasaka, R.; Tanaka, K.; Higashi, Y. Measurements of saturated densities and

- critical parameters for the binary mixture of 2,3,3,3-tetrafluoropropene (R-1234yf) + difluoromethane (R-32). *Int. J. Refrig.* **2013**, *36*, 1341–1346, DOI: 10.1016/j.ijrefrig.2013.02.005.
- (87) Cai, X.-D.; Zhang, N.; Chen, L.-X.; Hu, P.; Zhao, G.; Liu, M.-H. Gaseous PvTx measurements of HFO-1234yf + HFC-32 binary mixture by single-sinker magnetic suspension densimeter. *Fluid Phase Equilib.* **2018**, *460*, 119–125, DOI: 10.1016/j.fluid.2017.12.037.
- (88) Yang, J.; Jia, X.; Wu, J. Vapor phase pvTx measurements of binary mixtures of difluoromethane (R32) and 2,3,3,3-tetrafluoroprop-1-ene (R1234yf). *J. Chem. Thermodyn.* **2019**, *134*, 41–51, DOI: 10.1016/j.jct.2019.02.028.
- (89) Jia, X.; Yang, J.; Wu, J. Compressed liquid densities of binary mixtures of difluoromethane (R32) and 2,3,3,3-tetrafluoroprop-1-ene (R1234yf) at temperatures from (283 to 363) K and pressures up to 100 MPa. *J. Chem. Thermodyn.* **2020**, *141*, 105935, DOI: 10.1016/j.jct.2019.105935.
- (90) Tomassetti, S.; Coccia, G.; Pierantozzi, M.; Di Nicola, G.; Brown, J. S. Vapor phase and two-phase PvTz measurements of difluoromethane + 2,3,3,3-tetrafluoroprop-1-ene. *J. Chem. Thermodyn.* **2020**, *141*, 105966, DOI: 10.1016/j.jct.2019.105966.
- (91) Kobayashi, K.; Tanaka, K.; Higashi, Y. Measurements of the Critical Locus for HFO-1234ze(E) + HFC-32 Mixture. The 31st Japan Symposium on Thermophysical Properties. Fukuoka: Japan, 2010.
- (92) Yamaya, K.; Matsuguchi, A.; Kagawa, N. Study on the Isochoric Specific Heat Capacity of a R32+R1234ze(E) Mixture in the Liquid Phase. 23rd IIR International Congress of Refrigeration. Prague: Czech Republic, 2011.
- (93) Jia, T.; Bi, S.; Hu, X.; Meng, X.; Wu, J. Volumetric properties of binary mixtures of (difluoromethane (R32) + trans-1,3,3,3-tetrafluoropropene (R1234ze(E))) at temperatures from 283.15 K to 363.15 K and pressures up to 100 MPa. *J. Chem. Thermodyn.* **2016**, *101*, 54–63, DOI: 10.1016/j.jct.2016.05.013.
- (94) Tomassetti, S.; Perera, U. A.; Di Nicola, G.; Pierantozzi, M.; Higashi, Y.; Thu, K. Two-Phase and Vapor-Phase Thermophysical Property (pvTz) Measurements of the Difluoromethane + trans-1,3,3,3-Tetrafluoroprop-1-ene Binary System. *J. Chem. Eng. Data* **2020**, *65*, 1554–1564, DOI: 10.1021/acs.jced.9b00995.
- (95) Tomassetti, S.; Di Nicola, G.; Pierantozzi, M.; Brown, J. S. Two-Phase and Vapor Phase PvTx Properties of the Difluoromethane + cis-1,3,3,3-Tetrafluoroprop-1-ene Binary System. *J. Chem. Eng. Data* **2020**, *65*, 4326–4334, DOI: 10.1021/acs.jced.0c00334.
- (96) Mondéjar, M. E.; McLinden, M. O.; Lemmon, E. W. Thermodynamic Properties of trans-1-Chloro-3,3,3-trifluoropropene (R1233zd(E)): Vapor Pressure, (p , ρ , T) Behavior, and Speed of Sound Measurements, and Equation of State. *J. Chem. Eng. Data* **2015**, *60*, 2477–2489, DOI: 10.1021/acs.jced.5b00348.
- (97) Gao, N.; Chen, G.; Wang, Y.; Tang, L. Experimental isobaric heat capacity of liquid HFC-32 + HFO-1234ze(E) mixture and extension of a predictive corresponding state equation to HFC mixtures. *Int. J. Refrig.* **2018**, *88*, 318–323, DOI: 10.1016/j.ijrefrig.2018.02.015.
- (98) Schmid, B.; Gmehling, J. Revised parameters and typical results of the VTPR group contribution equation of state. *Fluid Phase Equilib.* **2012**, *317*, 110–126, DOI: 10.1016/j.fluid.2012.01.006.

- (99) Schmid, B.; Gmehling, J. Present status of the group contribution equation of state VTPR and typical applications for process development. *Fluid Phase Equilib.* **2016**, *425*, 443–450, DOI: 10.1016/j.fluid.2016.06.042.
- (100) Schmid, B.; Schedemann, A.; Gmehling, J. Extension of the VTPR group contribution equation of state: Group interaction parameters for additional 192 group combinations and typical results. *Ind. Eng. Chem. Res.* **2014**, *53*, 3393–3405, DOI: 10.1021/ie404118f.
- (101) Su, W.; Zhou, S.; Zhao, L.; Zhou, N. Vapor–Liquid Equilibrium Prediction of Refrigerant Mixtures with Peng–Robinson Equation of State and Binary Interaction Parameters Calculated Through Group Contribution Model. *Int. J. Thermophys.* **2020**, *41*, 14, DOI: 10.1007/s10765-019-2592-3.
- (102) Bell, I.; Welliquet, J.; Mondejar, M.; Bazyleva, A.; Quoilin, S.; Haglind, F. Application of the group contribution volume translated Peng–Robinson equation of state to new commercial refrigerant mixtures. *Int. J. Refrig.* **2019**, *103*, 316–328, DOI: 10.1016/j.ijrefrig.2019.04.014.
- (103) Fouad, W. A.; Alasiri, H. Molecular dynamic simulation and SAFT modeling of the viscosity and self-diffusion coefficient of low global warming potential refrigerants. *J. Mol. Liq.* **2020**, *317*, 113998, DOI: 10.1016/j.molliq.2020.113998.
- (104) Lötgering-Lin, O.; Fischer, M.; Hopp, M.; Gross, J. Pure Substance and Mixture Viscosities Based on Entropy Scaling and an Analytic Equation of State. *Ind. Eng. Chem. Res.* **2018**, *57*, 4095–4114, DOI: 10.1021/acs.iecr.7b04871.
- (105) Liu, H.; Yang, F.; Yang, Z.; Duan, Y. Modeling the viscosity of hydrofluorocarbons, hydrofluoroolefins and their binary mixtures using residual entropy scaling and cubic-plus-association equation of state. *J. Mol. Liq.* **2020**, *308*, 113027, DOI: 10.1016/j.molliq.2020.113027.
- (106) Kontogeorgis, G. M.; Folas, G. K. *Thermodynamic Models for Industrial Applications: From Classical and Advanced Mixing Rules to Association Theories*; Wiley, 2010.
- (107) Qian, J.-W.; Privat, R.; Jaubert, J.-N.; Coquelet, C.; Ramjugernath, D. Fluid-phase-equilibrium prediction of fluorocompound-containing binary systems with the predictive E-PPR78 model. *Int. J. Refrig.* **2017**, *73*, 65–90, DOI: <https://doi.org/10.1016/j.ijrefrig.2016.09.013>.
- (108) Lemmon, E. W.; Tillner-Roth, R. A Helmholtz energy equation of state for calculating the thermodynamic properties of fluid mixtures. *Fluid Phase Equilib.* **1999**, *165*, 1–21, DOI: 10.1016/S0378-3812(99)00262-9.
- (109) Lemmon, E. W.; Jacobsen, R. T. A Generalized Model for the Thermodynamic Properties of Mixtures. *Int. J. Thermophys.* **1999**, *20*, 825–835, DOI: 10.1023/A:1022627001338.
- (110) Raabe, G. Molecular Modeling of Fluoropropene Refrigerants. *J. Phys. Chem. B* **2012**, *116*, 5744–5751, DOI: 10.1021/jp300991t.
- (111) Raabe, G. Purely Predictive Vapor–Liquid Equilibrium Properties of 3,3,4,4,4-Pentafluoro-1-butene (HFO-1345fz), 2,3,3,4,4,4-Hexafluoro-1-butene (HFO-1336yf), and trans-1-Chloro-2,3,3,3-tetrafluoropropene (HCFO-1224yd(E)) from Molecular Simulation. *J. Chem. Eng. Data* **2020**, *65*, 4318–4325, DOI: 10.1021/acs.jced.0c00325.

- (112) Raabe, G. Molecular simulation studies in hydrofluoroolefine (HFO) working fluids and their blends. *Sci. Tech. Built Env.* **2016**, *22*, 1077–1089, DOI: 10.1080/23744731.2016.1206796.
- (113) Raabe, G. Molecular simulation studies on refrigerants past - present - future. *Fluid Phase Equilib.* **2019**, *485*, 190–198, DOI: 10.1016/j.fluid.2018.12.022.
- (114) Raabe, G. Molecular Simulation Studies on the Vapor-Liquid Phase Equilibria of Binary Mixtures of R-1234yf and R-1234ze(E) with R-32 and CO₂. *J. Chem. Eng. Data* **2013**, *58*, 1867–1873, DOI: 10.1021/je4002619.
- (115) Lemmon, E. W.; Bell, I. H.; Huber, M. L.; McLinden, M. O. NIST Standard Reference Database 23: Reference Fluid Thermodynamic and Transport Properties-REFPROP, Version 10.0, National Institute of Standards and Technology. <http://www.nist.gov/srd/nist23.cfm>, 2018.
- (116) Bell, I. H.; Wronski, J.; Quoilin, S.; Lemort, V. Pure and Pseudo-pure Fluid Thermophysical Property Evaluation and the Open-Source Thermophysical Property Library CoolProp. *Ind. Eng. Chem. Res.* **2014**, *53*, 2498–2508, DOI: 10.1021/ie4033999.
- (117) Bell, I. H.; Lemmon, E. W. Automatic Fitting of Binary Interaction Parameters for Multi-fluid Helmholtz-Energy-Explicit Mixture Models. *J. Chem. Eng. Data* **2016**, *61*, 3752–3760, DOI: 10.1021/acs.jced.6b00257.
- (118) Lemmon, E. W.; McLinden, M. O. Method for Estimating Mixture Equation of State Parameters. Thermophysical Properties and Transfer Processes of New Refrigerants, Paderborn, Germany. 2001.
- (119) Bell, I. H.; Deiters, U. K. On the construction of binary mixture *p-x* and *T-x* diagrams from isochoric thermodynamics. *AIChE J.* **2018**, *64*, 2745–2757, DOI: 10.1002/aic.16074.
- (120) Bell, I. H.; McLinden, M. O. The Status of Thermodynamic Data and Models for CF₃I and its Mixtures. *Int. J. Thermophys.* **2020**, *41*, 134, DOI: 10.1007/s10765-020-02712-w.
- (121) Tkaczuk, J.; Bell, I. H.; Lemmon, E. W.; Luchier, N.; Millet, F. Equations of State for the Thermodynamic Properties of Binary Mixtures for Helium-4, Neon, and Argon. *J. Phys. Chem. Ref. Data* **2020**, *49*, 023101, DOI: <https://doi.org/10.1063/1.5142275>.
- (122) Deiters, U. K.; Bell, I. H. Calculation of Critical Curves of Fluid Mixtures through Solution of Differential Equations. *Ind. Eng. Chem. Res.* **2020**, *59*, 19062–19076, DOI: 10.1021/acs.iecr.0c03667.
- (123) Bell, I. H.; Jäger, A. Calculation of critical points from Helmholtz-energy-explicit mixture models. *Fluid Phase Equilib.* **2017**, *433*, 159–173, DOI: 10.1016/j.fluid.2016.10.030.
- (124) van Konynenburg, P. H.; Scott, R. L. Critical Lines and Phase Equilibria in Binary Van Der Waals Mixtures. *Philos. T. R. Soc. A* **1980**, *298*, 495–540, DOI: 10.1098/rsta.1980.0266.
- (125) Privat, R.; Jaubert, J.-N. Classification of global fluid-phase equilibrium behaviors in binary systems. *Chem. Eng. Res. Des.* **2013**, *91*, 1807–1839, DOI: <https://doi.org/10.1016/j.cherd.2013.06.026>.
- (126) Beckmüller, R.; Thol, M.; Bell, I. H.; Lemmon, E. W.; Span, R. New Equations of State for Binary Hydrogen Mixtures Containing Methane, Nitrogen, Carbon Monoxide, and Carbon Dioxide. *J. Phys. Chem. Ref. Data* **2021**, *50*, 013102, DOI: 10.1063/5.0040533.